Hormonal and spatial control of SUMOylation in the human and mouse adrenal cortex

Typhanie Dumontet, Isabelle Sahut-barnola, Damien Dufour, Anne-Marie Lefrançois-Martinez, Annabel Berthon, Nathanaëlle Montanier, Bruno Ragazzon, Cyril Djari, Jean-christophe Pointud, Florence Roucher-boulez, et al.

Hormonal and spatial control of SUMOylation in the human and mouse adrenal cortex

Typhanie Dumontet[1], Isabelle Sahut-Barnola[1], Damien Dufour[1], Anne-Marie Lefrançois-Martinez[1], Annabel Berthon[1], Nathanaëlle Montanier[1,2], Bruno Ragazzon[3], Cyril Djari[1], Jean-Christophe Pointud[1], Florence Roucher-Boulez[1,4], Marie Batisse-Lignier[1,5], Igor Tauveron[1,5], Jérôme Bertherat[3,6], Pierre Val[1] and Antoine Martinez[1*]

[1] GReD, Université Clermont-Auvergne, CNRS, INSERM, F-63001 Clermont-Ferrand, FRANCE

[2] Service d'Endocrinologie, CHR, Hôpital de la Source, F-45100 Orléans, FRANCE

[3] Institut Cochin, Université Paris Descartes, CNRS, INSERM, F-75014 Paris, France.

[4] Endocrinologie Moléculaire et Maladies Rares, CHU, Université Claude Bernard Lyon 1, F-69677 Bron, FRANCE.

[5] Service d'Endocrinologie, Faculté de Médecine, CHU, Université Clermont-Auvergne, 63000 Clermont-Ferrand, FRANCE

[6] Centre Maladies Rares de la Surrénale, Service d'Endocrinologie, Hôpital Cochin, Assistance Publique Hôpitaux de Paris, F-75014 Paris, FRANCE.

*Address correspondence to Antoine Marinez, Université Clermont-Auvergne, GReD, CNRS UMR6293, INSERM U1103, Faculté de Médecine, CRBC, 28 place Henri Dunant, BP38, 63001 Clermont-Ferrand, France. Phone: 33.4.73.40.74.09; Fax: 33.4.40.70.42; Email: antoine.martinez@uca.fr

Running title: PKA coordinates SUMOylation in adrenal cortex

The authors have declared that no conflict of interest exists.

ABBREVIATIONS

ACTH	Adrenocorticotropin hormone
AKR1B7	Aldo-keto reductase 1B7
ATC1	Adrenocortical tumor cell line 1
cAMP	cyclic adenosine monophosphate
CBX4	Chromobox 4
CNC	Carney complexe syndrome
CRE	Cyclisation recombinase
CREB	Cyclic AMP responsive element binding protein
CRTC	CREB regulated transcription coactivator
CTNNB1	β-catenin
DESI1	DeSUMOylating isopeptidase 1
HPA	Hypothalamo-pituitary-adrenal axis
LOH	Loss-of-heterozygosity
NSE2	SMC5-6 (structural maintenance of chromosome 5-6) complex SUMO ligase
NURR1	Nuclear receptor related-1 protein (NR4A2)
PIAS1-4	Protein inhibitor of activated STAT-1 (signal transducer and activator of transcription-1) 1-4
PKA	Protein kinase cAMP-dependent
PPNAD	Primary pigmented nodular adrenocortical disease
RANBP2	Ran GTPase binding protein 2
RANGAP1	Ran GTPase activating protein 1
R1α/ PRKAR1A	PKA-dependent type 1 regulatory subunit α/gene
RSPO	R-spondin
RT-qPCR	quantitative reverse transcription polymerase chain reaction
SAE1/2	SUMO-activating enzyme subunit 1/2
SENP1-7	SUMO/sentrin specific peptidase 1-7
SF-1	Steroidogenic factor-1 (NR5A1)
SIK	Salt inducible kinase
SUMO	Small ubiquitin-like modifier
WNT	Wingless-related integration site
UBE2I	Ubiquitin conjugating enzyme E2 I

WT	Wild-type
WT1	Wilms tumor protein 1
zF	zona fasciculata
zG	zona glomerulosa
zR	zona reticularis

ABSTRACT

SUMOylation is a highly conserved and dynamic post-translational mechanism primarily affecting nuclear programs for adapting organisms to stressful challenges. Alteration of SUMOylation cycles leads to severe developmental and homeostatic defects and malignancy, but signals coordinating SUMOylation are still unidentified. The adrenal cortex is a zonated endocrine gland that controls body homeostasis and stress response. Here we show that in human and in mouse adrenals, SUMOylation follows a decreasing centripetal gradient that mirrors cortical differentiation flow and delimits highly- and weakly SUMOylated steroidogenic compartments, overlapping glomerulosa and fasciculata zones. Activation of PKA signalling by acute hormonal treatment, mouse genetic engineering or in Carney complex disease results in repression of SUMO conjugation in the inner cortex by coordinating expression of SUMO pathway inducers and repressors. Conversely, genetic activation of canonical WNT signalling maintains high SUMOylation potential in the outer neoplastic cortex. Thus, SUMOylation is tightly regulated by signalling pathways that orchestrate adrenal zonation and diseases.

KEY WORDS: Endocrine diseases . PKA . SENP1/2 . PIAS3. β-catenin . mouse models

INTRODUCTION

The adrenal cortex is divided into structurally and functionally distinct concentric zones (1). Under the capsule, the *zona glomerulosa* (zG) is formed by a narrow layer of cells arranged in rosettes that ensure production of aldosterone under the control of angiotensin II and potassium, mainly through calcium signalling (2). The *zona fasciculata* (zF*)*, located just below, forms a wide layer of cells arranged in radial columns responsible for the secretion of glucocorticoids, in response to ACTH, acting through cAMP/PKA signalling pathway (3). The *zona reticularis* (zR), located in the inner part of the cortex close to the medulla, is composed of cells organized in networks. It forms during adrenarche (around 7 years in humans) and supports the secretion of adrenal androgen precursors in response to ACTH (4). These zones constitute the definitive/adult cortex. In rodents, the adult cortex only consists of zG and zF (5). However, in mouse, a third and transient zone termed the X-zone is located in the innermost part of the cortex, and is considered as a remnant of the fetal cortex (6, 7). By its capacity to rapidly release hormones acting both on blood pressure control and glucido-lipidic metabolism, the adrenal gland is considered as the endocrine gland for stress response.

The zonal organization and cellular renewal of the adrenal cortex are maintained throughout life by a centripetal mechanisms involving the recruitment of progenitor cells from the periphery of the gland that migrate inward and differentiate successively into zG and zF cells (8, 9). Hormonal signals that control adrenal function not only ensure homeostatic maintenance but also participate to the zonation of the cortex. The Rspo/Wnt/β-catenin signalling pathway contributes to the acquisition of zG identity (10, 11) whereas ACTH/cAMP/PKA signalling is essential for zF and zR differentiation (12, 13). Maintaining adequate zonation during the unidirectional renewal of the cortex is ensured at least by the antagonistic interactions between these two signalling pathways and through epigenetic programming of newly recruited cells (14–16).

PKA (Protein Kinase A) is a tetramer composed of two catalytic and two cAMP-binding regulatory subunits. When intracellular levels of cAMP increase, following activation of the G protein coupled ACTH receptor, the regulatory subunits release the catalytic subunits which become active and phosphorylate downstream effectors (17). These targets include transcription factors stimulating the expression of steroidogenic genes. Inactivating mutations of the *PRKAR1A* gene encoding the regulatory subunit R1α lead to constitutive activation of PKA and development of Carney complex, a multiple endocrine neoplasia syndrome (18, 19). Primary Pigmented Nodular Adrenocortical Disease (PPNAD), the most frequent endocrine tumor in these patients is a benign adrenal hyperplasia, responsible for ACTH-independent hypercortisolism (Cushing's syndrome) (20). We have shown that the adrenal inactivation of *Prkar1a* in developing mice is sufficient to induce ACTH-independent Cushing's syndrome and formation of apoptosis-resistant hyperplasia in the inner zF (21, 22). Moreover, by tracing the lineage of *Prkar1a* mutant cells in the adult gland, we have established that PKA signalling is a driving force for sexually dimorphic cortex replenishment and for the conversion of zF into zR identity (13).

SUMOylation has emerged as a critical mechanism for modulating fundamental cellular and developmental processes, whose dysregulation can lead to severe diseases. Its involvement in tissue morphogenesis (23) has been demonstrated in enterocytes (24), keratinocytes (25) and adipocytes (26, 27). However, it also participates in human malignancy by favouring cancer cell stemness (28, 29). Post-translational modification of proteins by the covalent addition of SUMO1-3 (Small Ubiquitin-like Modifier) peptides requires an enzymatic cascade involving the E1 Sae1/Sae2 heterodimer for activation step, the Ube2i (Ubc9) E2 enzyme for conjugation step, and E3 ligation enzymes including Pias1-4, RanBP2, Nse2 and Cbx4 proteins (30). The dynamics and reversibility of the reaction are ensured by Senp1-7 and Desi1 proteases that cleave SUMO peptides from their substrates (31, 32).

One of the major roles of SUMOylation cycles is the control of transcription processes through the individual modification of trans-acting factors and chromatin remodelling (33–35). The properties of the transcription factors WT1, Nurr1 and SF-1 that are essential for development and function of adrenal cortex, are also regulated by SUMOylation (36–40). However, physiological evidence of the impact of SUMOylation on adrenal cortex function remains scarce but was elegantly brought into light by knock-in experiment from H. Ingraham's group (41). Indeed, the complete lack of SUMO-conjugated SF-1 in mice expressing a unSUMOylatable $Sf1^{2KR}$ allele was shown to affect adrenal zonation (delayed X-zone regression), expanded the progenitor compartment, disturbed cell identities (ectopic gonadal traits) and resulted in mild endocrine hypofunction. This highlighted the importance of SF-1 SUMOylation in fine-tuning the genetic programs of endocrine differentiation but our knowledge of overall SUMOylation patterns in the adrenal gland and hormonal regulation of this process is still lacking. Interestingly, increased cAMP levels was shown to influence the expression of members of the SUMO pathway in ovarian granulosa cells (42).

Here, we hypothesized that SUMOylation, cortex architecture and hormonal regulation of adrenocortical function should be coordinated. To test this hypothesis, we analysed the influence of ACTH/PKA signalling on the SUMOylation process in cell culture, wild-type mice, genetic mouse models of adrenal diseases and in human PPNAD tissues. This enabled us to propose that cell signallings critical for adrenal cortex homeostasis and stress response tighly coordinate the SUMOylation pathway which in turn is found altered in cortical diseases.

MATERIALS AND METHODS

Adrenocortical cell cultures. Adrenocortical Tumor Cells 1 were established from an adrenal tumor derived from a mouse expressing the SV40 T antigen under the control of the *Akr1b7* promoter specific to the adrenal cortex (AdTAg mouse) (43, 44). The primary cultures were obtained from adrenals of female mice aged of 3 weeks following the protocol described above (45). The cells were cultured on poly-D-lysine-coated dishes (Sigma-Aldrich) in a DMEM-F12 medium (Life Technologies SAS.) At 37 ° C. in the presence of 5% CO_2, insulin (10 µg/mL), transferrin (5.5 µg/mL), selenium (6.7 ng/mL) (ITS, Life Technologies SAS), L-glutamine (2mM), penicillin 0.1U/ml), streptomycin (0.1 µg/mL), 2.5% horse serum and 2.5% fetal calf serum (43). For PKA induction experiments, cells were seeded in 6-well plates at a density of 2.10^5 cells per well, cultured to subconfluence and then weaned 12h (serum-free medium) prior to the addition of forskolin, ACTH, cycloheximide, actinomycin, at the times and concentrations indicated in the legends of the Fig.s.

Animals and treatments. Two-month-old SWISS CD-1 mice received an i.p. injection of immediate ACTH (0.05 mg/30 g, Synacthene® 0.25 mg/mL, Novartis Pharma S.A.) 2h or 4h before adrenal sampling. Others received i.m. injection of long-acting ACTH (12 µg/30 g, Synacthene Retard 1 mg/mL, Novartis Pharma S.A) and the adrenals were dissected 6h or 24h later. For the 24h point, the mice received a second injection 12h before sampling. Immediate ACTH, with a short half-life, allows to observe the early effects of stimulation. The delayed ACTH is stabilized because complexed with zinc salts, the diffusion is slowed which allows to observe effects in the longer term. Alternatively, 6-month-old females were injected s.c. with dexamethasone 21-acetate for 5 days in order to deplete endogenous ACTH production (75 µg twice daily in corn oil) and were injected with immediate ACTH for 2h or 6h. The female *Sf1-Cre::Prkar1a*$^{fl/fl}$ and ΔCat (*Akr1b7-Cre::Catnb*$^{lox(ex3)}$) mice used were 2.5- and 18-month-old, respectively (11, 14). The mice were sacrificed by decapitation and the adrenals immediately frozen in liquid nitrogen.

Protein extraction and western blot. Cell and tissue samples were lysed in RIPA (Radio Immunoprecipitation Assays) buffer (50 mM Tris-HCl, pH7.4, 1% NP40, 0.25% Na-deoxycholate, 150 mM NaCl, 1 mM EDTA) supplemented extemporaneously with phosphatase inhibitors (1 mM Na_3VO_4, 0.5 mM NaF), protease inhibitors (Roche Diagnostics) and SUMO inhibitors proteases N-ethylmaleimide (NEM, Sigma-Aldrich) (3.13 mg/mL). The cell debris was removed by centrifugation at 13,000 rpm for 15 minutes at 4 °C. The protein concentration was determined by the Bradford method (Bio-Rad) and 50 µg of proteins were denatured for 5 minutes at 95 ° C in Læmmli (50 mM Tris, 100 mM DTT, 2% SDS, 0.1% Bromophenol blue, 12% glycerol). The proteins were then separated on a 7% SDS-PAGE (Fig. 2D) or precast gels 4-15% (BioRad) (Supplemental Fig. S3D) and transferred to a nitrocellulose membrane (Hybond ECL, Amersham Biosciences) overnight at 4 °C at 50V

followed by one hour at 120V. Non-specific protein binding sites were saturated for 1h at room temperature by incubation in TBS-T (50 mM Tris-HCl (pH 8), 150 mM NaCl and 0.1% Tween 20) containing 5% Regilait®. Incubation with the appropriate primary antibody (Supplemental Table S1A) was carried out in the same buffer overnight at 4 °C with gentle stirring. After rinsing in TBS-T, the membranes were incubated for 1h at room temperature with the appropriate secondary antibody conjugated with peroxidase. The specific complexes were revealed by chemiluminescence (ECL) system (Enhancer chemoluminescent, Amersham). The fluorescence signals were quantified using the MultiGauge V 3.2 software.

RT-qPCR analyses. The cell samples were lysed in Trizol (Invitrogen) and the total RNAs were extracted according to the manufacturer's recommendations. Tissue samples were ground in RNA II lysis buffer (Macherey Nagel) and total RNAs were extracted using the NucleoSpin RNA II kit as recommended by the manufacturer. Five hundred nanograms of mRNA were reverse-transcribed for 1h at 37 ° C with 5 pmoles (reverse transcriptase), 2.5 mM dNTP and 20 units of RNAse inhibitors (recombinant RNAsin, N2615, Promega) in a final volume of 25 µL. The cDNAs obtained were used (at 1/4 dilution) as template for RT-qPCR analysis using the qPCR SYBR (TAKRR820W, Takara) premix under standard conditions (40 cycles at 95 °C for 15 sec, 60 °C for 15 sec and 72°C for 20 sec). The relative accumulation of mRNAs was determined from the average of duplicates by the ΔΔCt method (46), using the *Actin* household gene. The primers are listed in Supplemental Table S1B.

Immunohistochemistry. After collection, the adrenals were fixed in 4% PFA for 24 hours, dehydrated in an increasing gradient of ethanol and then placed in Histoclear (HS200, National Diagnostics, Atlanta, USA) for 2 h before being included in paraffin. 5 µm thick sections were made using a microtome (HM 340E, ThermoFisher Scientific, Massachusetts, USA). The tissue sections were then dewaxed by passing through the Histoclear and progressively rehydrated in an increasing gradient of ethanol. Immunohistological analyses were performed according to the conditions described in Supplemental Table S1C. The tissues were photographed using an Axioplan2 Imaging microscope (Zeiss, Jena, Germany). In order to evaluate the presence of non-SUMOylated nuclei, a counter-staining with haematoxylin was performed on the same sections previously used for SUMO1 immunohistochemistry. Quantification of SUMO signals were performed using Zen Software (Zeiss).

Patients. Adrenal tissue analysis and genetic diagnosis was obtained from patients after signed consent. The study was approved by an institutional review committee (Advisory Committee for the Protection of Persons in Biomedical Research, Cochin Hospital, Paris). PPNAD paraffin sections were performed from adrenal samples

of PPNAD patients who underwent bilateral adrenalectomy for ACTH-independent Cushing's syndrome. Most patients were carriers of *PRKAR1A* inactivating germinal mutations.

Statistical analysis. Statistical analyses were performed using a Student t-test or Mann-Witney test depending on Gaussian values distribution to compare two groups. For multiple comparisons, one way ANOVA (Gaussian values distribution) test or Kruskal-Wallis (non-Gaussian values distribution) test followed by Dunett's, Dunn's or Tukey post hoc tests were performed. A p-value of less than or equal to 0.05 was considered statistically significant. (*$p \leq 0.05$, **$p \leq 0.01$, ***$p \leq 0.001$, ****$p \leq 0.0001$).

Study approval. All animal work was conducted according to French and European directives for the use and care of animals for research purposes and was approved by the local ethics committee, C2E2A (Comité d'Ethique pour l'Expérimentation Animale en Auvergne).

RESULTS

SUMO conjugation is repressed by ACTH/PKA signalling in adrenocortical cells *in vitro*.

To evaluate the role of PKA signalling on adrenocortical proteins SUMOylation, we analysed the effects of forskolin, an adenylate cyclase activator, on the formation of SUMO conjugates in lysates of ATC1 mouse adrenocortical cells (43). Immunoblotting with either anti-SUMO1 (Fig. 1A) or anti-SUMO2/3 (Fig. 1B) showed that sumoylated proteins in cell extracts were represented by a smear of bands of high molecular mass whose intensity decreased with forskolin, reaching a nadir after 6h-12h treatment. Quantification of the western-blots showed that steady-state levels of Sumo1- and Sumo2/3-conjugated proteins were reduced by 54% and 40%, respectively, after 6h of forskolin treatment.

To explore the mechanism leading to PKA-mediated inhibition of protein SUMOylation, the hormonal responsiveness of genes encoding SUMO modules and enzymes of the SUMO conjugation/deconjugation pathway (Fig. 1C) was assessed by RTqPCR, in ATC1 cell line and primary adrenocortical cells (Fig. 1D). In both cell types, strong induction of *Akr1b7* mRNA levels, a well characterised ACTH/PKA-responsive gene (43), validated treatments at all time-points, including the expected more robust effect of forskolin compared to ACTH, the physiological inducer (Supplemental Fig. S1A). In both cell culture systems, PKA stimulation downregulated mRNA accumulation of *Sumo1*, *Sae1*, *Pias3* and, to a lesser extent, *Ube2i,* with a maximal effect occurring between 6h and 12h (Fig. 1D). Conversely, these treatments induced a two-fold increase in *Senp2* mRNA expression that culminated between 2-6h. This positive PKA responsiveness was also observed at protein levels (Fig. 1E) suggesting that *Senp2* gene regulation by ACTH/PKA was mainly transcriptional as confirmed by the sensitivity to actinomycin D and resistance to cycloheximide (Supplemental Fig. S1B). Mechanisms of PKA-dependent repression of genes involved in SUMO conjugation (*Sumo1*, *Ube2i*, *Sae1* and *Pias3*) were less clear, but presumably required *de novo* expression of a labile repressor as suggested by *Pias3* mRNA sensitivity to both actinomycin D and cycloheximide (Supplemental Fig. S1B). Interestingly, although *Ube2i* transcripts levels were still elevated 6 hours post-induction in ATC1 cells, protein levels declined between 2 and 6h (Fig. 1E). Therefore, this further suggested that PKA-dependent repression might also be achieved by post-translational mechanisms. The responsiveness of the other effectors of SUMOylation appeared either unaffected by PKA stimulation or not reproduced under ACTH treatment (Supplemental Fig. S1C). Taken together these results indicate that PKA-induced overall decrease of SUMO-conjugated protein substrates in adrenocortical cells could be the consequence of two coordinated and convergent mechanisms: increased gene transcription of deSUMOylating enzyme (here *Senp2*) and repression of genes encoding SUMOylating proteins including SUMO peptides.

Acute and chronic effects of ACTH/PKA repress SUMOylation in mouse adrenal glands.

To evaluate in vivo, the hormonal responsiveness of genes of the SUMO-conjugation or -deconjugation pathways, WT young adult mice were injected with rapid- or long-acting forms of ACTH and sacrificed after 2-4h or 6-24h, respectively. RT-qPCR analyses in the adrenal cortex showed that activation of PKA signalling repressed mRNA levels of *Sumo1*, *Sumo2* and *Sumo3* by 50%, 25% and 30%, after 4h of treatment, respectively (Fig. 2A,B). Extended ACTH treatments showed that this decline was transient and could be maintained over 6h. However, expression re-increased at 24h (Supplemental Fig. S2A). A similar repression pattern was observed for *Pias3* mRNA levels that reached a nadir after 2-4h of treatment (75% drop) and re-increased at 24h (Fig. 2B and supplemental Fig. S2A). In contrast, transcripts levels for the SUMO protease *Senp2* were increased by two-fold after 2h, returning to pre-treatment values after 4h (Fig. 2B). Remarkably, mRNA levels for SUMO protease Desi1 remained stable for the first 6h of treatment and were increased more than 1.5-fold after 24h (Fig. 2B and supplemental Fig. S2A). Regardless of the treatment duration, the expression of *Ube2i* transcripts was unaltered (Fig. 2B and supplemental Fig. S2A). We next investigated the effect of chronic activation of PKA signalling on genes ensuring SUMO conjugation/deconjugation dynamics. For this, we used *Sf1-Cre::Prkar1a*$^{fl/fl}$ mice with adrenal-specific deletion of PKA regulatory R1α subunit (14). RT-qPCR analysis revealed a 38% reduction of *Pias3* expression compared to wild-type levels while *Senp2* and *Desi1* expression was induced by 1.5- and 2-fold, respectively. *Senp3* and *Senp5* mRNA levels also showed a modest but significant increase (Fig. 2C). Interestingly, under these chronic stimulation conditions, there was no downregulation of *Sumo* genes and expression levels of all other conjugating/deconjugating genes were unaltered or only slightly increased (Supplemental Fig. S2B). In agreement with the repression of *Pias3* and simultaneous stimulation of genes for deSUMOylating isopeptidases, western-blot analysis of adrenal lysates showed that Sumo2/3 conjugation levels in mutant mice were approximately 30% of wild-type (Fig. 2D).

Taken together, these data suggest that ACTH stimulation in vivo, limits the SUMOylation process in the adrenal gland through both acute (≤4h) and chronic (≥24h) transcriptional effects. These lead to the simultaneous and opposite regulation of a subset of PKA-responsive genes of the SUMOylation pathway, with repression of actors of the conjugation process (*Sumo1-3* and *Pias3*), and stimulation of deconjugation enzymes (*Senp2, Senp3, Senp5* and *Desi1*).

Regionalisation of SUMOylation in the adrenal cortex is dependent on ACTH/PKA signalling.

In the adrenal cortex, ACTH/PKA signalling is required for differentiation, maintenance and function of the zF (12, 13). Active SUMOylation processes can be assessed in tissue sections by monitoring changes in the intensity of nuclear SUMO signal (47, 48). Immunohistochemical staining of mouse adrenal samples revealed a cortical gradient of Sumo1 and Sumo2/3 staining in steroidogenic cells, with high nuclear signal in the peripheral subcapsular/glomerulosa region, intermediate signal at the glomerulosa-fasciculata junction and low labelling in fasciculata cells (Fig. 3A,B & supplemental Fig. S3A). Sumo1 and Sumo2/3 staining pattern was

similar in both sexes although the decrease SUMOylation levels between zG to zF appeared more pronounced in females (Supplemental Fig. S3B). Interestingly, SUMO labelling was not restricted to steroidogenic cells. Indeed, capsular as well as endothelial cell nuclei were strongly positive for Sumo2/3 whereas Sumo1 staining was much less pronounced in these cell populations (Fig. 3A,B & supplemental Fig. S3B).

In order to evaluate the consequences of changes in the hypothalamic-pituitary adrenal (HPA) axis on SUMO staining profile, mice were either treated for 5 days with dexamethasone to block endogenous ACTH secretion, or supplemented with (rapid-acting) ACTH injection on the last day (Fig. 3C). Compared to basal conditions, HPA axis blockade had no significant effect on either Sumo1 or Sumo2/3 nuclear staining patterns. In contrast, ACTH supplementation resulted in a transient decrease in SUMO nuclear labelling that affected all cortical zones after 2h and almost returned to pre-treatment labelling after 6h. Interestingly, the negative effect of ACTH was restricted to steroidogenic cells since nuclear Sumo2/3 staining intensity was unaltered in capsular or endothelial cells. In agreement with histological data, western blotting analysis of the corresponding adrenal extracts showed a parallel change of Sumo2/3 and Sumo1 conjugate levels (Supplemental Fig. S3D). General staining pattern for SUMO was also assessed in adrenal sections from *Sf1-Cre::Prkar1a*$^{fl/fl}$ mice. This showed that chronic stimulation of PKA signalling in the cortex resulted in the relative loss of centripetal gradient of nuclear Sumo1 labelling typical of WT cortex (Supplemental Fig. S3C). Altogether, these results indicate that there is a centripetally decreasing gradient of SUMOylation throughout adrenal cortical zones that relies on the activity of ACTH/PKA signalling, which maintains relative hypoSUMOylation context in steroidogenic cells of the zF.

Differential SUMOylation pattern of adrenal cortex is conserved in human adrenal and is altered in primary pigmented nodular adrenal hyperplasia (PPNAD) from Carney complex patients.

To assess whether our observations were transferable to human, we analysed by immunohistochemistry, the SUMOylation pattern of adrenal samples from either healthy patients or from hypercortisolic patients suffering from pathological activation of PKA due to Carney complex disease (CNC). The SUMO1 and SUMO2/3 immunolabelling performed on normal human adrenal sections revealed a centripetally decreasing gradient of steroidogenic cells nuclear staining intensity similar to that found in mice (Fig. 4A & supplemental Fig. S4A). Accordingly, nuclear staining intensity was maximal in cells of the outer cortex (zG and zG/zF transition zone) and weaker in the zF and zR. Interestingly, SUMO1 immunolabelling of adrenal samples from CNC patients (n=3+3), revealed obvious hypoSUMOylation of cells forming the hyperplastic nodules (as evidenced by hematoxylin counterstaining). This contrasted with the intense SUMO1 nuclear staining found in adjacent internodular tissue (Fig. 4B & supplemental Fig. S4B). Reciprocally, the signal for SUMO protease SENP1 was more pronounced within nodules (Fig. 4C & supplemental Fig. S4C). Altogether, these data suggested that the SUMOylation potential was inhibited in a context of constitutive PKA activity due to R1α loss within

PPNAD nodules (*PRKAR1A* LOH) and was maintained or even increased in a context of blunted PKA activity, as found in the atrophic internodular fasciculata tissue (due to repressed ACTH levels (49)). We conclude that as suggested by mice studies, SUMOylation follows a centripetal decreasing gradient in human adrenal cortex that seems to negatively correlate with activation of PKA signalling in normal gland (zF) and in adrenal nodules from patients suffering from CNC.

WNT/β-catenin signalling favours SUMOylation in the adrenal cortex.

We have previously established that WNT and PKA signalling pathways exert complementary and antagonistic actions to maintain adrenal cortex zonation: WNT signalling is essential for zG identity, whereas PKA signalling drives identity of the inner cortex (zF and zR) (13, 14). Therefore, we hypothesized that relative hyperSUMOylation of the outer cortex could rely on WNT/β-catenin signalling. To evaluate this hypothesis, we analysed changes in SUMO and β-catenin immunofluorescent staining in adrenal sections of ΔCat mice that present stochastic constitutive activation of β-catenin due to *Ctnnb1* exon 3 excision (*Akr1b7-Cre::Catnb*$^{fl(ex3)}$) (11)(Fig. 5A). As previously described, constitutive activation of WNT signalling resulted in expansion of the nucleo-cytoplasmic staining of β-catenin beyond zG and throughout the cortex. This resulted in formation of large hyperplastic cells clusters (Fig. 5B) in which β-catenin staining intensity was massively increased compared to the adjacent non-recombined tissue (Supplemental Fig. S5A). Co-immunofluorescent detection of either Sumo1 or Sumo2/3, revealed that hyperplastic clusters (β-catenin positive) and areas with highest Sumo nuclear labelling overlap. This was confirmed by quantifying Sumo nuclear signals in hyperplastic area (β-catenin high) and intact adjacent cortex (β-catenin low). This showed that increased SUMOylation correlated with β-catenin activation (Fig. 5C & 5D). We assessed possible concurrent changes in SUMO pathway gene expression in ΔCat adrenal glands using RT-qPCR. As illustrated in Fig. 5E, mRNA levels for genes involved in SUMO conjugation (*Sumo2*, *Sumo3*, *Pias1* and *Pias2*) were induced, while mRNA expression of SUMO protease *Desi1* was reduced by 50% in adrenals from ΔCat mice. With the exception of genes for SUMO protease *Senp1* and *Senp6* which were upregulated, expression of all other tested genes was unaltered in ΔCat adrenals (Supplemental Fig. S5B). We conclude that WNT/β-catenin signalling pathway activation favours SUMOylation *in vivo* and can participate in establishing the centripetally decreasing gradient of SUMOylation in the adrenal cortex by maintaining high SUMOylation potential in the outer cortex.

DISCUSSION

The results presented here show that there is a negative correlation between the activation of PKA signalling (genetically or hormonally induced) and the SUMOylation of adrenocortical proteins in cell culture and in vivo. This PKA-dependent hypoSUMOylation relies on the coordinated transcriptional stimulation of deSUMOylating isopeptidase genes (Senp2, Desi1, SENP1) and repression of genes encoding SUMO peptides and SUMO (Pias3) ligase. In agreement with this inhibitory effect, we show that in both human and mouse adrenal cortices, the SUMOylation pattern appears as a centripetal decreasing gradient. This is inversely correlated with PKA sensitivity of the cells, as emphasised by strong nuclear staining in zG and weaker staining in zF/zR. Activation of PKA signalling by ACTH injections leads to a transient decrease in SUMOylation in zF, which suggests a possible active role of this post-translational modification in zonation and/or stress response. Conversely, this gradient seems less sensitive to ACTH suppression as dexamethasone treatment leads to a slight though nonsignificant increased SUMOylation (Supplemental Fig. S3D). Moreover, the hypoSUMOylating effect of PKA signalling could participate in the aetiology of PPNAD. Indeed, we show that global SUMOylation is reduced in the nodules of patients with PPNAD as well as in the adrenals of a mouse model of PPNAD (*Sf1-Cre::Prkar1a*$^{fl/fl}$).

In adrenocortical cells, kinetics of SUMO pathway genes expression in response to PKA stimulation are similar to that of steroidogenic genes (43). This observation suggests that the SUMOylation process may be subordinated to the same regulatory mechanisms as steroidogenesis. Although PKA-mediated transcriptional activation is well documented, data on mechanisms relaying its repressive effects are scarce, even though they are quite prominent. Indeed, our transcriptome analyses of mice with adrenal *Prkar1a* gene inactivation with various Cre drivers (13, 14) showed similar numbers of down- and upregulated genes, following constitutive PKA activation. The only negative molecular mechanism identified to date in the adrenal gland, mobilizes the oscillating SIK-CRTC (Salt inducible kinase-CREB regulated transcription coactivator) cascade in which SIK represses the activity of CREB in a transient PKA-dependent manner (50–52). The participation of SIK-CRTC in the transcriptional repression of *Sumo1-3* and *Pias3* genes will require further investigation.

In contrast to SUMO conjugating genes, and in agreement with the overall hypoSUMOylation induced by PKA, expression of deSUMOylases Senp2 and Desi1 is stimulated by activation of PKA signalling, in the same way as steroidogenic genes. The induction of *Senp2* mRNA expression by ACTH/PKA might rely on the recruitment of CREB to a functional cAMP responsive element (CRE) located in the proximal promoter region that was described to mediate PKA responsiveness in 3T3L1 preadipocytes (53). No functional data are available for the *Desi1* regulatory regions although several putative CREs are predicted by bioinformatics (not shown). However, the kinetics of ACTH responsiveness in vivo, with fast up-regulation of *Senp2* transcripts (2h) and slow up-regulation of *Desi1* (24h), suggests that mechanisms contributing to their regulation by PKA may

differ. In addition, Senp2 and Desi1 proteins are supposed to diverge in their subcellular localization. Indeed, whereas Senp2 is mainly nuclear (54) Desi1 is cytoplasmic (32). This suggests that their target substrates may differ.

The centripetal decreasing gradient of SUMOylation within the adrenal cortex (zG>zF/zR) together with its sensitivity to the HPA axis, are suggestive of a role for SUMOylation in the response to stress. Accordingly, requirement of SUMO pathway for adaptative response to stress seems to have been conserved in evolution (55). Indeed, proteomic analyses have demonstrated the coordinated SUMOylation of protein groups involved in the same biochemical pathway after genotoxic stress in yeast (56). SENP2-dependent deSUMOylation is required to adapt cells to etoposide-induced genotoxic stress while SENP1-mediated deSUMOylation is required to counteract colon tumour growth, induced by genotoxic E. coli strains (57, 58). In agreement with this concept, the repressor effect of PKA signalling on the SUMOylation process could participate in the transcriptional response of adrenocortical cells following stress. The constitutive hypoSUMOylation in zF could exert a permissive action on the response to stress, by lifting the "tonic" repression exerted by SUMOylation on transcription factors such as SF-1 and Nurr1 (37, 59). Under stress conditions, ACTH-induced transient hypoSUMOylation would further facilitate steroidogenic response. Furthermore, activation of some PDEs following their SUMOylation (60), suggests that such an intracellular feedback mechanism would allow the adrenal cortex to sustain elevated intracellular levels of cAMP and promote activation of PKA. The hypoSUMOylation observed in PPNAD nodules suggests the involvement of this modification in the aetiology of the disease. These results are consistent with the increasing number of studies involving SUMOylation in tumour mechanisms (61).

Finally, the decreasing gradient of SUMOylation in the adrenal cortex also suggests its possible involvement in the establishment and/or maintenance of cortical zonation. Increased SUMOylation consecutive to depletion of SENP1/2/7 proteins was reported in various models, to activate the WNT/β-catenin pathway by increasing β-catenin stability (62, 63) and by promoting its nuclear translocation (64, 65). The ability of SUMOylation to activate the WNT pathway is likely to explain the intense staining observed in zG. Reciprocally, we report here that constitutive β-catenin activation in mouse adrenals, not only induces zG tumour formation (11, 66) but also expands the hyperSUMOylation domain. This suggests that a positive feedback loop between SUMO-induced WNT pathway and β-catenin-dependent SUMOylation increase could allow maintaining higher SUMO staining in the zG. Conversely, the hypoSUMOylating effects of PKA signalling activation could participate (*e.g.* through *Senp2/SENP1* upregulated expression) in the antagonism between WNT/β-catenin and ACTH/PKA pathways, which is needed to establish proper functional zonation and to counteract β-catenin-induced tumour formation (13, 14).

In conclusion, our findings reveal that protein SUMOylation follows a conserved centripetal decreasing gradient within the adrenal cortex. This relies on antagonistic actions of ACTH/PKA and WNT/β-catenin signalling

pathways: ACTH/PKA signalling acutely reduces SUMOylation in zF by coordinating the expression of both SUMO pathway inducers and repressors, whereas WNT/β-catenin induces hypersumoylation. Our data suggest that programming of the SUMOylation pattern could play a role in endocrine function and stress response, maintenance of zonation and pathology (hypersecretion syndromes and cancer).

ACKNOWLEDGMENTS

We also wish to thank Sandrine Plantade, Philippe Mazuel and Khirredine Ouchen for care of the transgenic mice. We thank Kaitlin J. Basham (University of Michigan) for critical reading of the manuscript. This work was funded through institutional support from Centre national de la Recherche Scientifique, Institut National de la Santé et de la Recherche Médicale, Université Clermont-Auvergne, the French government IDEX-ISITE initiative 16-IDEX-0001 (CAP 20-25) and supported by grants from Région Auvergne-Rhône-Alpes to T.D., from Fondation Association pour la Recherche sur le Cancer to T.D., from Agence Nationale pour la Recherche (ANR-14-CE12-000) to A.M.

AUTHOR CONTRIBUTION

TD, ISB, DD, AMLM, PV, and AM conceived and designed the experiments; TD, ISB, DD, AMLM, AB, NM, CD, JCP and FRB performed the experiments; TD, ISB, DD, AMLM and AM analysed the data; BR, MBL, IT and JB provided human samples; AM supervised the project, and TD and AM wrote the paper; PV and all authors edited the paper.

REFERENCES

1. Vinson, G. P. (2016) Functional Zonation of the Adult Mammalian Adrenal Cortex. *Front. Neurosci.* **10**, 238
2. Bollag, W. B. (2014) Regulation of aldosterone synthesis and secretion. *Compr. Physiol.* **4**, 1017–1055
3. Gorrigan, R. J., Guasti, L., King, P., Clark, A. J., and Chan, L. F. (2011) Localisation of the melanocortin-2-receptor and its accessory proteins in the developing and adult adrenal gland. *J. Mol. Endocrinol.* **46**, 227–232
4. Auchus, R. J. and Rainey, W. E. (2004) Adrenarche - physiology, biochemistry and human disease. *Clin. Endocrinol. (Oxf.)* **60**, 288–296
5. Yates, R., Katugampola, H., Cavlan, D., Cogger, K., Meimaridou, E., Hughes, C., Metherell, L., Guasti, L., and King, P. (2013) Adrenocortical development, maintenance, and disease. *Curr. Top. Dev. Biol.* **106**, 239–312
6. Morohashi, K. and Zubair, M. (2011) The fetal and adult adrenal cortex. *Mol. Cell. Endocrinol.* **336**, 193–197
7. Zubair, M., Parker, K. L., and Morohashi, K. (2008) Developmental links between the fetal and adult zones of the adrenal cortex revealed by lineage tracing. *Mol Cell Biol* **28**, 7030–7040
8. Freedman, B. D., Kempna, P. B., Carlone, D. L., Shah, M. S., Guagliardo, N. A., Barrett, P. Q., Gomez-Sanchez, C. E., Majzoub, J. A., and Breault, D. T. (2013) Adrenocortical zonation results from lineage conversion of differentiated zona glomerulosa cells. *Dev Cell* **26**, 666–673
9. King, P., Paul, A., and Laufer, E. (2009) Shh signaling regulates adrenocortical development and identifies progenitors of steroidogenic lineages. *Proc Natl Acad Sci U A* **106**, 21185–21190
10. Vidal, V., Sacco, S., Rocha, A. S., da Silva, F., Panzolini, C., Dumontet, T., Doan, T. M. P., Shan, J., Rak-Raszewska, A., Bird, T., Vainio, S., Martinez, A., and Schedl, A. (2016) The adrenal capsule is a signaling center controlling cell renewal and zonation through Rspo3. *Genes Dev.* **30**, 1389–1394
11. Berthon, A., Sahut-Barnola, I., Lambert-Langlais, S., de Joussineau, C., Damon-Soubeyrand, C., Louiset, E., Taketo, M. M., Tissier, F., Bertherat, J., Lefrancois-Martinez, A. M., Martinez, A., and Val, P. (2010) Constitutive beta-catenin activation induces adrenal hyperplasia and promotes adrenal cancer development. *Hum Mol Genet* **19**, 1561–1576
12. Chida, D., Nakagawa, S., Nagai, S., Sagara, H., Katsumata, H., Imaki, T., Suzuki, H., Mitani, F., Ogishima, T., Shimizu, C., Kotaki, H., Kakuta, S., Sudo, K., Koike, T., Kubo, M., and Iwakura, Y. (2007) Melanocortin 2 receptor is required for adrenal gland development, steroidogenesis, and neonatal gluconeogenesis. *Proc Natl Acad Sci U A* **104**, 18205–18210
13. Dumontet, T., Sahut-Barnola, I., Septier, A., Montanier, N., Plotton, I., Roucher-Boulez, F., Ducros, V., Lefrançois-Martinez, A.-M., Pointud, J.-C., Zubair, M., Morohashi, K.-I., Breault, D. T., Val, P., and Martinez, A. (2018) PKA signaling drives reticularis differentiation and sexually dimorphic adrenal cortex renewal. *JCI Insight* **3**
14. Drelon, C., Berthon, A., Sahut-Barnola, I., Mathieu, M., Dumontet, T., Rodriguez, S., Batisse-Lignier, M., Tabbal, H., Tauveron, I., Lefrançois-Martinez, A.-M., Pointud, J.-C., Gomez-Sanchez, C. E., Vainio, S., Shan, J., Sacco, S., Schedl, A., Stratakis, C. A., Martinez, A., and Val, P. (2016) PKA inhibits WNT signalling in adrenal cortex zonation and prevents malignant tumour development. *Nat. Commun.* **7**, 12751
15. Mathieu, M., Drelon, C., Rodriguez, S., Tabbal, H., Septier, A., Damon-Soubeyrand, C., Dumontet, T., Berthon, A., Sahut-Barnola, I., Djari, C., Batisse-Lignier, M., Pointud, J.-C., Richard, D., Kerdivel, G., Calméjane, M.-A., Boeva, V., Tauveron, I., Lefrançois-Martinez, A.-M., Martinez, A., and Val, P. (2018) Steroidogenic differentiation and PKA signaling are programmed by histone methyltransferase EZH2 in the adrenal cortex. *Proc. Natl. Acad. Sci. U. S. A.* **115**, E12265–E12274
16. Walczak, E. M., Kuick, R., Finco, I., Bohin, N., Hrycaj, S. M., Wellik, D. M., and Hammer, G. D. (2014) Wnt signaling inhibits adrenal steroidogenesis by cell-autonomous and non-cell-autonomous mechanisms. *Mol. Endocrinol. Baltim. Md* **28**, 1471–1486
17. Sunahara, R. K., Dessauer, C. W., and Gilman, A. G. (1996) Complexity and diversity of mammalian

adenylyl cyclases. *Annu. Rev. Pharmacol. Toxicol.* **36**, 461–480
18. Carney, J. A., Gordon, H., Carpenter, P. C., Shenoy, B. V., and Go, V. L. (1985) The complex of myxomas, spotty pigmentation, and endocrine overactivity. *Med. Baltim.* **64**, 270–283
19. Kirschner, L. S., Carney, J. A., Pack, S. D., Taymans, S. E., Giatzakis, C., Cho, Y. S., Cho-Chung, Y. S., and Stratakis, C. A. (2000) Mutations of the gene encoding the protein kinase A type I-alpha regulatory subunit in patients with the Carney complex. *Nat Genet* **26**, 89–92
20. Bertherat, J., Horvath, A., Groussin, L., Grabar, S., Boikos, S., Cazabat, L., Libe, R., René-Corail, F., Stergiopoulos, S., Bourdeau, I., Bei, T., Clauser, E., Calender, A., Kirschner, L. S., Bertagna, X., Carney, J. A., and Stratakis, C. A. (2009) Mutations in regulatory subunit type 1A of cyclic adenosine 5'-monophosphate-dependent protein kinase (PRKAR1A): phenotype analysis in 353 patients and 80 different genotypes. *J. Clin. Endocrinol. Metab.* **94**, 2085–2091
21. Sahut-Barnola, I., de Joussineau, C., Val, P., Lambert-Langlais, S., Damon, C., Lefrancois-Martinez, A. M., Pointud, J. C., Marceau, G., Sapin, V., Tissier, F., Ragazzon, B., Bertherat, J., Kirschner, L. S., Stratakis, C. A., and Martinez, A. (2010) Cushing's syndrome and fetal features resurgence in adrenal cortex-specific Prkar1a knockout mice. *PLoS Genet* **6**, e1000980
22. de Joussineau, C., Sahut-Barnola, I., Tissier, F., Dumontet, T., Drelon, C., Batisse-Lignier, M., Tauveron, I., Pointud, J.-C., Lefrançois-Martinez, A.-M., Stratakis, C. A., Bertherat, J., Val, P., and Martinez, A. (2014) mTOR pathway is activated by PKA in adrenocortical cells and participates in vivo to apoptosis resistance in primary pigmented nodular adrenocortical disease (PPNAD). *Hum. Mol. Genet.* **23**, 5418–5428
23. Deyrieux, A. F. and Wilson, V. G. (2017) Sumoylation in Development and Differentiation. *Adv. Exp. Med. Biol.* **963**, 197–214
24. Demarque, M. D., Nacerddine, K., Neyret-Kahn, H., Andrieux, A., Danenberg, E., Jouvion, G., Bomme, P., Hamard, G., Romagnolo, B., Terris, B., Cumano, A., Barker, N., Clevers, H., and Dejean, A. (2011) Sumoylation by Ubc9 regulates the stem cell compartment and structure and function of the intestinal epithelium in mice. *Gastroenterology* **140**, 286–296
25. Deyrieux, A. F., Rosas-Acosta, G., Ozbun, M. A., and Wilson, V. G. (2007) Sumoylation dynamics during keratinocyte differentiation. *J. Cell Sci.* **120**, 125–136
26. Liu, B., Wang, T., Mei, W., Li, D., Cai, R., Zuo, Y., and Cheng, J. (2014) Small ubiquitin-like modifier (SUMO) protein-specific protease 1 de-SUMOylates Sharp-1 protein and controls adipocyte differentiation. *J. Biol. Chem.* **289**, 22358–22364
27. Liu, Y., Zhang, Y.-D., Guo, L., Huang, H.-Y., Zhu, H., Huang, J.-X., Liu, Y., Zhou, S.-R., Dang, Y.-J., Li, X., and Tang, Q.-Q. (2013) Protein inhibitor of activated STAT 1 (PIAS1) is identified as the SUMO E3 ligase of CCAAT/enhancer-binding protein β (C/EBPβ) during adipogenesis. *Mol. Cell. Biol.* **33**, 4606–4617
28. Zhang, Z., Du, J., Wang, S., Shao, L., Jin, K., Li, F., Wei, B., Ding, W., Fu, P., van Dam, H., Wang, A., Jin, J., Ding, C., Yang, B., Zheng, M., Feng, X.-H., Guan, K.-L., and Zhang, L. (2019) OTUB2 Promotes Cancer Metastasis via Hippo-Independent Activation of YAP and TAZ. *Mol. Cell* **73**, 7-21.e7
29. Cui, C.-P., Wong, C. C.-L., Kai, A. K.-L., Ho, D. W.-H., Lau, E. Y.-T., Tsui, Y.-M., Chan, L.-K., Cheung, T.-T., Chok, K. S.-H., Chan, A. C. Y., Lo, R. C.-L., Lee, J. M.-F., Lee, T. K.-W., and Ng, I. O. L. (2017) SENP1 promotes hypoxia-induced cancer stemness by HIF-1α deSUMOylation and SENP1/HIF-1α positive feedback loop. *Gut* **66**, 2149–2159
30. Geiss-Friedlander, R. and Melchior, F. (2007) Concepts in sumoylation: a decade on. *Nat. Rev. Mol. Cell Biol.* **8**, 947–956
31. Nayak, A. and Müller, S. (2014) SUMO-specific proteases/isopeptidases: SENPs and beyond. *Genome Biol.* **15**, 422
32. Shin, E. J., Shin, H. M., Nam, E., Kim, W. S., Kim, J.-H., Oh, B.-H., and Yun, Y. (2012) DeSUMOylating isopeptidase: a second class of SUMO protease. *EMBO Rep.* **13**, 339–346
33. Verger, A., Perdomo, J., and Crossley, M. (2003) Modification with SUMO. A role in transcriptional regulation. *EMBO Rep.* **4**, 137–142
34. Heun, P. (2007) SUMOrganization of the nucleus. *Curr. Opin. Cell Biol.* **19**, 350–355
35. Neyret-Kahn, H., Benhamed, M., Ye, T., Le Gras, S., Cossec, J.-C., Lapaquette, P., Bischof, O., Ouspenskaia, M., Dasso, M., Seeler, J., Davidson, I., and Dejean, A. (2013) Sumoylation at chromatin governs

coordinated repression of a transcriptional program essential for cell growth and proliferation. *Genome Res.* **23**, 1563–1579
36. Smolen, G. A., Vassileva, M. T., Wells, J., Matunis, M. J., and Haber, D. A. (2004) SUMO-1 modification of the Wilms' tumor suppressor WT1. *Cancer Res.* **64**, 7846–7851
37. Galleguillos, D., Vecchiola, A., Fuentealba, J. A., Ojeda, V., Alvarez, K., Gómez, A., and Andrés, M. E. (2004) PIASgamma represses the transcriptional activation induced by the nuclear receptor Nurr1. *J. Biol. Chem.* **279**, 2005–2011
38. Komatsu, T., Mizusaki, H., Mukai, T., Ogawa, H., Baba, D., Shirakawa, M., Hatakeyama, S., Nakayama, K. I., Yamamoto, H., Kikuchi, A., and Morohashi, K. (2004) Small ubiquitin-like modifier 1 (SUMO-1) modification of the synergy control motif of Ad4 binding protein/steroidogenic factor 1 (Ad4BP/SF-1) regulates synergistic transcription between Ad4BP/SF-1 and Sox9. *Mol Endocrinol* **18**, 2451–2462
39. Chen, W. Y., Lee, W. C., Hsu, N. C., Huang, F., and Chung, B. C. (2004) SUMO modification of repression domains modulates function of nuclear receptor 5A1 (steroidogenic factor-1). *J Biol Chem* **279**, 38730–38735
40. Lee, M. B., Lebedeva, L. A., Suzawa, M., Wadekar, S. A., Desclozeaux, M., and Ingraham, H. A. (2005) The DEAD-box protein DP103 (Ddx20 or Gemin-3) represses orphan nuclear receptor activity via SUMO modification. *Mol Cell Biol* **25**, 1879–1890
41. Lee, F. Y., Faivre, E. J., Suzawa, M., Lontok, E., Ebert, D., Cai, F., Belsham, D. D., and Ingraham, H. A. (2011) Eliminating SF-1 (NR5A1) sumoylation in vivo results in ectopic hedgehog signaling and disruption of endocrine development. *Dev Cell* **21**, 315–327
42. Yang, F. M., Pan, C. T., Tsai, H. M., Chiu, T. W., Wu, M. L., and Hu, M. C. (2009) Liver receptor homolog-1 localization in the nuclear body is regulated by sumoylation and cAMP signaling in rat granulosa cells. *FEBS J* **276**, 425–436
43. Ragazzon, B., Lefrancois-Martinez, A. M., Val, P., Sahut-Barnola, I., Tournaire, C., Chambon, C., Gachancard-Bouya, J. L., Begue, R. J., Veyssiere, G., and Martinez, A. (2006) Adrenocorticotropin-dependent changes in SF-1/DAX-1 ratio influence steroidogenic genes expression in a novel model of glucocorticoid-producing adrenocortical cell lines derived from targeted tumorigenesis. *Endocrinology* **147**, 1805–1818
44. Batisse-Lignier, M., Sahut-Barnola, I., Tissier, F., Dumontet, T., Mathieu, M., Drelon, C., Pointud, J.-C., Damon-Soubeyrand, C., Marceau, G., Kemeny, J.-L., Bertherat, J., Tauveron, I., Val, P., Martinez, A., and Lefrançois-Martinez, A.-M. (2017) P53/Rb inhibition induces metastatic adrenocortical carcinomas in a preclinical transgenic model. *Oncogene*
45. Lefrancois-Martinez, A.-M., Blondet-Trichard, A., Binart, N., Val, P., Chambon, C., Sahut-Barnola, I., Pointud, J.-C., and Martinez, A. (2011) Transcriptional control of adrenal steroidogenesis: novel connection between Janus kinase (JAK) 2 protein and protein kinase A (PKA) through stabilization of cAMP response element-binding protein (CREB) transcription factor. *J. Biol. Chem.* **286**, 32976–32985
46. Winer, J., Jung, C. K., Shackel, I., and Williams, P. M. (1999) Development and validation of real-time quantitative reverse transcriptase-polymerase chain reaction for monitoring gene expression in cardiac myocytes in vitro. *Anal. Biochem.* **270**, 41–49
47. Yang, W., Sheng, H., Warner, D. S., and Paschen, W. (2008) Transient focal cerebral ischemia induces a dramatic activation of small ubiquitin-like modifier conjugation. *J. Cereb. Blood Flow Metab. Off. J. Int. Soc. Cereb. Blood Flow Metab.* **28**, 892–896
48. Tirard, M., Hsiao, H.-H., Nikolov, M., Urlaub, H., Melchior, F., and Brose, N. (2012) In vivo localization and identification of SUMOylated proteins in the brain of His6-HA-SUMO1 knock-in mice. *Proc. Natl. Acad. Sci. U. S. A.* **109**, 21122–21127
49. Tirosh, A., Valdés, N., and Stratakis, C. A. (2018) Genetics of micronodular adrenal hyperplasia and Carney complex. *Presse Medicale Paris Fr. 1983* **47**, e127–e137
50. Lin, X., Takemori, H., Doi, J., Katoh, Y., and Okamoto, M. (2000) SIK (Salt-inducible kinase): regulation of ACTH-mediated steroidogenic gene expression and nuclear/cytosol redistribution. *Endocr. Res.* **26**, 995–1002
51. Takemori, H. and Okamoto, M. (2008) Regulation of CREB-mediated gene expression by salt inducible kinase. *J. Steroid Biochem. Mol. Biol.* **108**, 287–291

52. Jagannath, A., Butler, R., Godinho, S. I. H., Couch, Y., Brown, L. A., Vasudevan, S. R., Flanagan, K. C., Anthony, D., Churchill, G. C., Wood, M. J. A., Steiner, G., Ebeling, M., Hossbach, M., Wettstein, J. G., Duffield, G. E., Gatti, S., Hankins, M. W., Foster, R. G., and Peirson, S. N. (2013) The CRTC1-SIK1 pathway regulates entrainment of the circadian clock. *Cell* **154**, 1100–1111
53. Chung, S. S., Ahn, B. Y., Kim, M., Choi, H. H., Park, H. S., Kang, S., Park, S. G., Kim, Y. B., Cho, Y. M., Lee, H. K., Chung, C. H., and Park, K. S. (2010) Control of adipogenesis by the SUMO-specific protease SENP2. *Mol Cell Biol* **30**, 2135–2146
54. Hang, J. and Dasso, M. (2002) Association of the human SUMO-1 protease SENP2 with the nuclear pore. *J. Biol. Chem.* **277**, 19961–19966
55. Tempé, D., Piechaczyk, M., and Bossis, G. (2008) SUMO under stress. *Biochem. Soc. Trans.* **36**, 874–878
56. Psakhye, I. and Jentsch, S. (2012) Protein group modification and synergy in the SUMO pathway as exemplified in DNA repair. *Cell* **151**, 807–820
57. Lee, M. H., Mabb, A. M., Gill, G. B., Yeh, E. T. H., and Miyamoto, S. (2011) NF-κB induction of the SUMO protease SENP2: A negative feedback loop to attenuate cell survival response to genotoxic stress. *Mol. Cell* **43**, 180–191
58. Cougnoux, A., Dalmasso, G., Martinez, R., Buc, E., Delmas, J., Gibold, L., Sauvanet, P., Darcha, C., Déchelotte, P., Bonnet, M., Pezet, D., Wodrich, H., Darfeuille-Michaud, A., and Bonnet, R. (2014) Bacterial genotoxin colibactin promotes colon tumour growth by inducing a senescence-associated secretory phenotype. *Gut* **63**, 1932–1942
59. Campbell, L. A., Faivre, E. J., Show, M. D., Ingraham, J. G., Flinders, J., Gross, J. D., and Ingraham, H. A. (2008) Decreased recognition of SUMO-sensitive target genes following modification of SF-1 (NR5A1). *Mol Cell Biol* **28**, 7476–7486
60. Li, X., Vadrevu, S., Dunlop, A., Day, J., Advant, N., Troeger, J., Klussmann, E., Jaffrey, E., Hay, R. T., Adams, D. R., Houslay, M. D., and Baillie, G. S. (2010) Selective SUMO modification of cAMP-specific phosphodiesterase-4D5 (PDE4D5) regulates the functional consequences of phosphorylation by PKA and ERK. *Biochem. J.* **428**, 55–65
61. Seeler, J.-S. and Dejean, A. (2017) SUMO and the robustness of cancer. *Nat. Rev. Cancer* **17**, 184–197
62. Karami, S., Lin, F.-M., Kumar, S., Bahnassy, S., Thangavel, H., Quttina, M., Li, Y., Ren, J., and Bawa-Khalfe, T. (2017) Novel SUMO-Protease SENP7S Regulates β-catenin Signaling and Mammary Epithelial Cell Transformation. *Sci. Rep.* **7**, 46477
63. Huang, H.-J., Zhou, L.-L., Fu, W.-J., Zhang, C.-Y., Jiang, H., Du, J., and Hou, J. (2015) β-catenin SUMOylation is involved in the dysregulated proliferation of myeloma cells. *Am. J. Cancer Res.* **5**, 309–320
64. Choi, H.-K., Choi, K.-C., Yoo, J.-Y., Song, M., Ko, S. J., Kim, C. H., Ahn, J.-H., Chun, K.-H., Yook, J. I., and Yoon, H.-G. (2011) Reversible SUMOylation of TBL1-TBLR1 regulates β-catenin-mediated Wnt signaling. *Mol. Cell* **43**, 203–216
65. Tan, M., Gong, H., Wang, J., Tao, L., Xu, D., Bao, E., Liu, Z., and Qiu, J. (2015) SENP2 regulates MMP13 expression in a bladder cancer cell line through SUMOylation of TBL1/TBLR1. *Sci. Rep.* **5**, 13996
66. Berthon, A., Drelon, C., Ragazzon, B., Boulkroun, S., Tissier, F., Amar, L., Samson-Couterie, B., Zennaro, M. C., Plouin, P. F., Skah, S., Plateroti, M., Lefebvre, H., Sahut-Barnola, I., Batisse-Lignier, M., Assie, G., Lefrancois-Martinez, A. M., Bertherat, J., Martinez, A., and Val, P. (2014) WNT/beta-catenin signalling is activated in aldosterone-producing adenomas and controls aldosterone production. *Hum Mol Genet* **23**, 889–905

FIGURE LEGENDS

Fig. 1. Activation of PKA signalling decreases global SUMOylation in adrenocortical cell cultures. *A-B*) Time course effects of PKA activation on the accumulation of adrenocortical proteins conjugated to Sumo1 (*A*) and Sumo2/3 (*B*). Murine adrenocortical ATC1 cell line was treated with forskolin (10^{-5}M) for the indicated time (h) or with vehicle (DMSO) for the longest treatment time. The accumulation of Sumo1 and Sumo2/3 conjugates was analysed by western blot (representative Fig.) and quantified (histograms). Tubulin signal was used to normalise the quantification of SUMO signals. *C*) Schematic representation of the SUMOylation cycle. Sumo1, Sumo2 and Sumo3 peptides are conjugated to their substrate proteins by an enzymatic process involving E1, E2 and E3 enzymes. The dynamism of the SUMOylation is ensured by the proteases Senp and Desi1 which allow the removal of the SUMO peptide from the targeted protein. *D*) Time course effects of PKA activation on the mRNA expression of SUMOylation pathway genes. Primary cultured cells from mouse adrenal cortex and ATC1 cell line were treated with forskolin (10^{-5}M) for the indicated time or with DMSO (Vhl) for the longest treatment time. Primary cultures were also treated with ACTH (10^{-9}M). RT-qPCR analyses were normalised with respect to Actin gene expression. *E*) PKA responsiveness of Senp2 and Ube2i protein levels. ATC1 cells were treated with forskolin (10^{-5}M) for the indicated time (h) or with DMSO (Vhl) for the longest treatment time. Protein accumulation of Senp2 and Ube2i was analysed by western blot. Tubulin signal serves as loading control. Quantification histograms represent mean ± SEM from 3-4 experiments. Statistical analyses were conducted by 1-way ANOVA followed by Dunett's test. *p<0.05; **p<0.01; ***p<0.005.

Fig. 2. Acute hormonal induction or constitutive activation of PKA signalling affect protein SUMOylation and SUMO pathway gene expression in mouse adrenals. *A-B*) Wild-type mice were injected with immediate ACTH and adrenals were removed 2h or 4h later, control adrenals were dissected from untreated mice (0h) and subjected to RNA extraction. *A*) Experimental setup. *B*) RT-qPCR analyses of SUMOylation pathway gene expression normalised with respect to *Actin* gene expression. Statistical analyses were conducted by 1-way ANOVA followed by Dunett's test. *C-D*) Carney complex mouse model with constitutive activation of PKA following adrenal inactivation of *Prkar1a* (*Sf1-Cre::Prkar1a*$^{fl/fl}$ mice). *C*) Experimental setup. Adrenals from *Sf1-Cre::Prkar1a*$^{+/+}$ (*WT*) and *Sf1-Cre::Prkar1a*$^{fl/fl}$ (*KO*) mice were removed and subjected to RNA and protein extraction. RT-qPCR analyses of SUMOylation pathway gene expression normalised with respect to *Actin* gene expression and, *D*) western blot analyses of Sumo2/3 conjugates in adrenal protein extracts and quantification (histogram). Tubulin signal was used to normalise the quantification of SUMO signals. Statistical analyses were conducted by Student t-test. Quantification histograms represent mean ± SEM. *p<0.05; **p<0.01; ***p<0.001.

Fig. 3. SUMOylation is regionalised in mouse adrenal cortex and modulated by ACTH/PKA signalling. *A-B*) SUMOylation profile forms a decreasing gradient of intensity from the outer to the inner cortex. The accumulation of conjugated proteins to Sumo1 (*A*) and Sumo2/3 (*B*) was analysed by immunohistochemistry in adrenals of 6-month-old female mice. The quantification graphs represent mean ± SEM of SUMO nuclear staining intensity in each histological zone and inter-zone all along the cortex and in medulla, for 3 adrenals from 3 different animals and 50-60 nuclei per adrenal. Statistical analyses were conducted by Kruskal-Wallis followed by Dunn's test. Ca: capsule; zG: zona glomerosa; zF^{ext}: external zona fasciculata; zF^{int}: internal zona fasciculata; M: medulla. *C*) Stimulation of the corticotropic axis changes the cortical SUMOylation profile. Six-month-old female mice were treated with dexamethasone (Dex.) for 5 days, injected or not the last morning with ACTH and sacrificed 2h or 6h later. Basal conditions correspond to untreated mice. The accumulation of conjugated nuclear proteins to Sumo1 and Sumo2/3 was analysed by immunohistochemistry. The quantification graphs represent mean ± SEM of SUMO nuclear staining intensity in zF cells for 6 adrenals from 6 different animals and 10 nuclei per adrenal. Black and white arrows: nuclear Sumo staining in capsular and endothelial cells, respectively. Statistical analyses were conducted by 1-way ANOVA followed by Tukey post hoc test. *p<0.05, **p<0.01, ***p<0.001, ****p<0.0001. Scale bars = 50 µm.

Fig. 4. SUMOylation is regionalized in human adrenal cortex and altered in nodular hyperplasia from Carney complex patients. *A*) SUMOylation profile forms a decreasing gradient of intensity from the outer to the inner cortex. The accumulation of conjugated proteins to SUMO1 was analysed by immunohistochemistry in a control human adrenal. The quantification graph represents mean ± SEM of SUMO1 nuclear staining intensity in steroidogenic cells in each histological zone and inter-zone all along the cortex. Statistical analyses were conducted by 1-way ANOVA followed by Dunett's test. ***p<0.001. zG: zona glomerosa, zF: zona fasciculata; zR: zona reticularis. *B-C*) HypoSUMOylation of PPNAD nodules. PPNAD sections from patients with *PRKAR1A* germinal mutation were immunostained for SUMO1 (*B*) or for SENP1 (*C*) and counterstained with hematoxylin (H&E). HypoSUMOylated nuclei (black arrow). N: nodule. Blue scale bars = 2 cm, black scale bars = 100 µm.

Fig. 5. Adrenal cortex SUMOylation is enhanced by constitutive activation of WNT/β-catenin signalling. *A*) Experimental setup. β-catenin stabilization in adrenal cortex was allowed by deletion of exon 3 of *Ctnnb1 (*$Catnb^{lox(ex3)}$ *allele)* using *Akr1b7-Cre* line (referred to as ΔCat mice). *B*) Coimmunofluorescent labeling of Sumo1 (upper) or Sumo2/3 (bottom) (green), β-catenin (red) and merged signals, in adrenal sections from ΔCat female mice of 18 months. *Inset*, magnification view showing nuclei from cells with low (white arrowheads) or high (white asterisk) β-catenin staining. Scale bars = 20 µm. *C*) The quantification graphs represent mean ± SEM of SUMO nuclear Sumo1 and Sumo2/3 staining intensity in cells that express low or high levels of β-

catenin (3 adrenals from 3 different animals and 10-15 nuclei per adrenal). *D*) Sumo1 or Sumo2/3 nuclear staining is correlated with β-catenin activation. Spearman correlation between staining intensity values of Sumo1 or Sumo2/3 nuclear signal and staining intensity of β-catenin nucleo-cytoplasmic signal. r: Spearman correlation coefficient. *E*) Adrenals from *Akr1b7-Cre::Catnb*$^{+/+}$ *(WT)* and *Akr1b7-Cre::Catnb*$^{lox(ex3)/+}$ (Δ*Cat*) mice were removed and subjected to RNA extraction. RT-qPCR analyses of SUMOylation pathway gene expression normalised with respect to *Actin* gene expression. Statistical analyses were conducted by Student t-test. Quantification histograms represent mean ± SEM. *p<0.05, **p<0.01, ***p<0.001

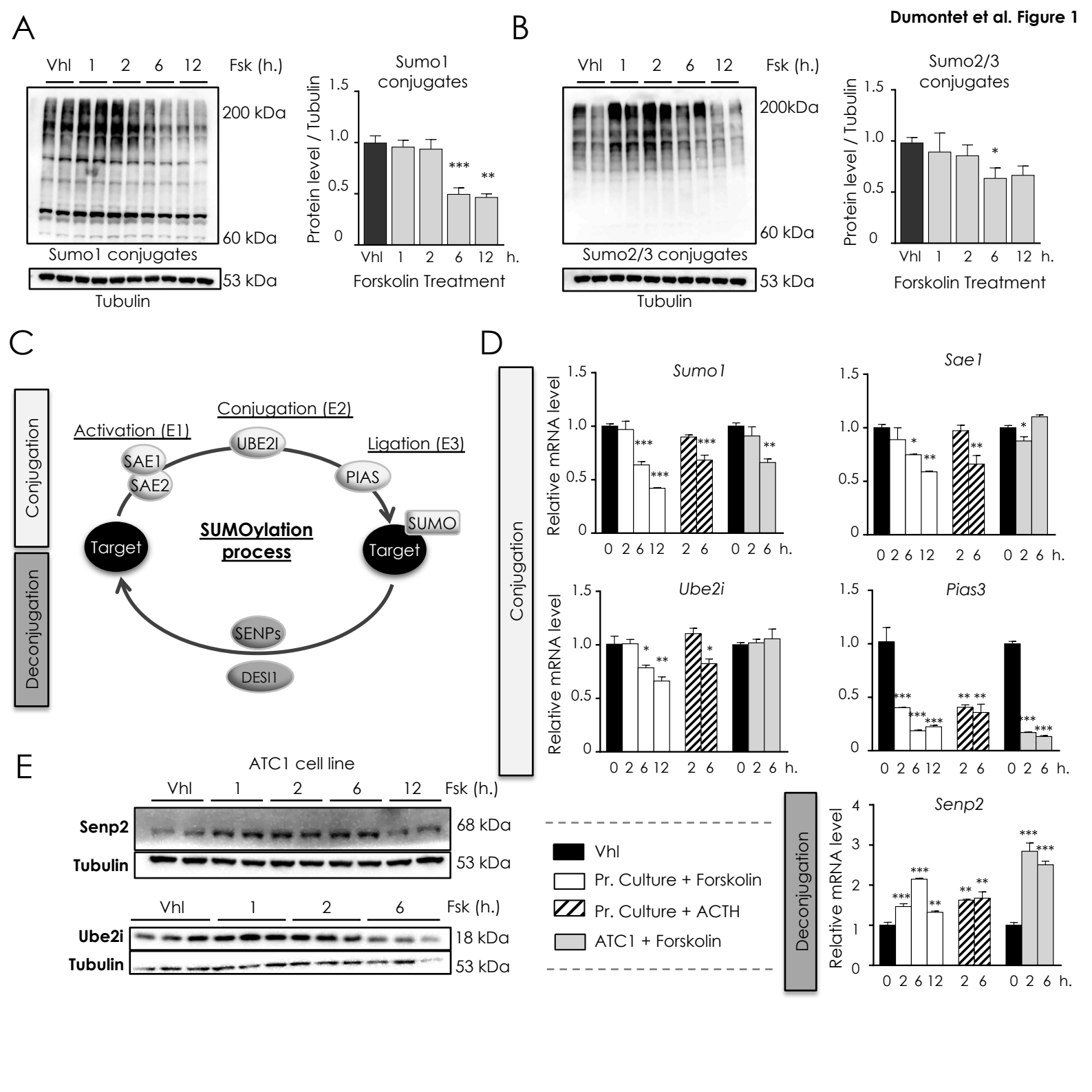
A
Vhl 1 2 6 12 Fsk (h.)
200 kDa
60 kDa
Sumo1 conjugates
53 kDa
Tubulin
Sumo1 conjugates
Protein level / Tubulin
Vhl 1 2 6 12 h.
Forskolin Treatment
B
Vhl 1 2 6 12 Fsk (h.)
200kDa
60 kDa
Sumo2/3 conjugates
53 kDa
Tubulin
Sumo2/3 conjugates
Protein level / Tubulin
Vhl 1 2 6 12 h.
Forskolin Treatment
C
Conjugation
Deconjugation
Activation (E1)
Conjugation (E2)
Ligation (E3)
SAE1
SAE2
UBE2I
PIAS
SUMO
Target
SUMOylation process
Target
SENPs
DESI1
D
Conjugation
Sumo1
Sae1
Ube2i
Pias3
Relative mRNA level
0 2 6 12 2 6 0 2 6 h.
E
ATC1 cell line
Vhl 1 2 6 12 Fsk (h.)
Senp2
68 kDa
Tubulin
53 kDa
Vhl 1 2 6 Fsk (h.)
Ube2i
18 kDa
Tubulin
53 kDa
Vhl
Pr. Culture + Forskolin
Pr. Culture + ACTH
ATC1 + Forskolin
Deconjugation
Senp2
Relative mRNA level
0 2 6 12 2 6 0 2 6 h.

Fig. 1. Activation of PKA signalling decreases global SUMOylation in adrenocortical cell cultures. *A-B*) Time course effects of PKA activation on the accumulation of adrenocortical proteins conjugated to Sumo1 (*A*) and Sumo2/3 (*B*). Murine adrenocortical ATC1 cell line was treated with forskolin (10^{-5}M) for the indicated time (h) or with vehicle (DMSO) for the longest treatment time. The accumulation of Sumo1 and Sumo2/3 conjugates was analysed by western blot (representative Fig.) and quantified (histograms). Tubulin signal was used to normalise the quantification of SUMO signals. *C*) Schematic representation of the SUMOylation cycle. Sumo1, Sumo2 and Sumo3 peptides are conjugated to their substrate proteins by an enzymatic process involving E1, E2 and E3 enzymes. The dynamism of the SUMOylation is ensured by the proteases Senp and Desi1 which allow the removal of the SUMO peptide from the targeted protein. *D*) Time course effects of PKA activation on the mRNA expression of SUMOylation pathway genes. Primary cultured cells from mouse adrenal cortex and ATC1 cell line were treated with forskolin (10^{-5}M) for the indicated time or with DMSO (Vhl) for the longest treatment time. Primary cultures were also treated with ACTH (10^{-9}M). RT-qPCR analyses were normalised with respect to Actin gene expression. *E*) PKA responsiveness of Senp2 and Ube2i protein levels. ATC1 cells were treated with forskolin (10^{-5}M) for the indicated time (h) or with DMSO (Vhl) for the longest treatment time. Protein accumulation of Senp2 and Ube2i was analysed by western blot. Tubulin signal serves as loading control. Quantification histograms represent mean ± SEM from 3-4 experiments. Statistical analyses were conducted by 1-way ANOVA followed by Dunett's test. *p<0.05; **p<0.01; ***p<0.005.

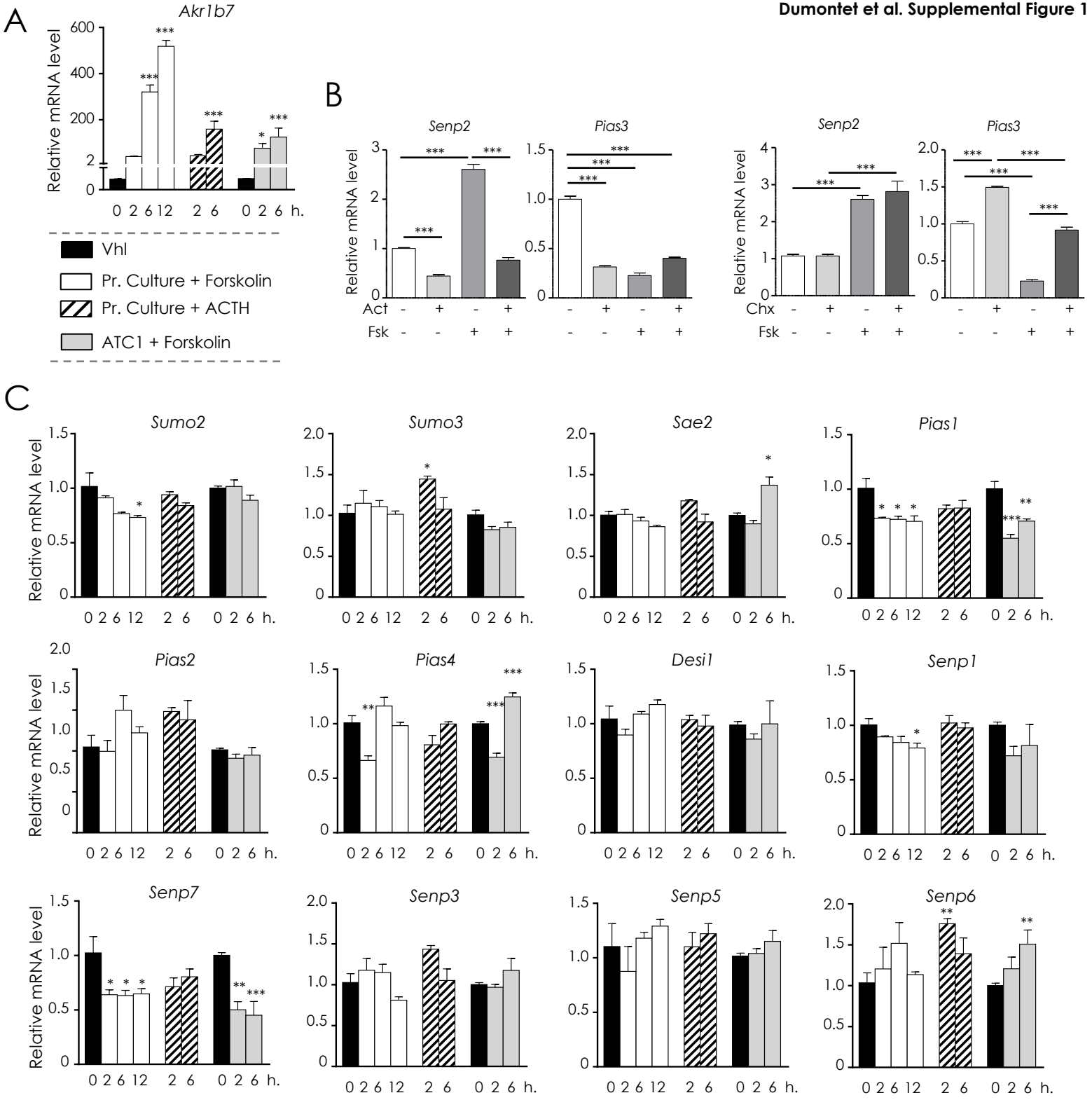
A
Akr1b7
Relative mRNA level
600
400
200
2
0
0 2 6 12 2 6 0 2 6 h.
Vhl
Pr. Culture + Forskolin
Pr. Culture + ACTH
ATC1 + Forskolin
B
Senp2
Pias3
Relative mRNA level
Act
Fsk
Chx
C
Sumo2
Sumo3
Sae2
Pias1
Pias2
Pias4
Desi1
Senp1
Senp7
Senp3
Senp5
Senp6

Supplemental Fig. S1. *A*) RT-qPCR analysis of *Akr1b7* transcripts was used as a control for PKA responsiveness of the cell cultures. Adrenocortical primary cultures and ATC1 cell line were treated with forskolin (10^{-5}M) for the indicated time (h) or with the vehicle DMSO (Vhl) for the longest treatment time. Primary cultures were also treated with ACTH (10^{-9}M). RT-qPCR analyses were normalised with respect to *Actin* gene expression. *B*) Comparison of *Senp2* and *Pias3* gene mRNA expression in ATC1 line in response to 2h induction with forskolin (Fsk) alone or in combination with actinomycin D (Act) or cycloheximide (Chx) at 10^{-5}M, at 1µg/mL and 10^{-5}M, respectively. Relative quantification of the transcripts of *Senp2* and *Pias3*. The transcripts were quantified by RT-qPCR and normalisation was performed with respect to *Actin* gene expression. *C*) Time course effects of PKA activation on the expression of *Sumo2/3 genes* and genes involved in E1 activation step (*Sae2*), E3 ligation step (*Pias1, 2, 4*) and deconjugation (*Senp1, 3, 5, 6, 7*). RT-qPCR analyses were normalised with respect to *Actin* gene expression. Quantification histograms represent mean ± SEM from 3-4 experiments. Statistical analyses were conducted by 1-way ANOVA followed by Dunett's test. *p<0.05; **p<0.01; ***p<0.005.

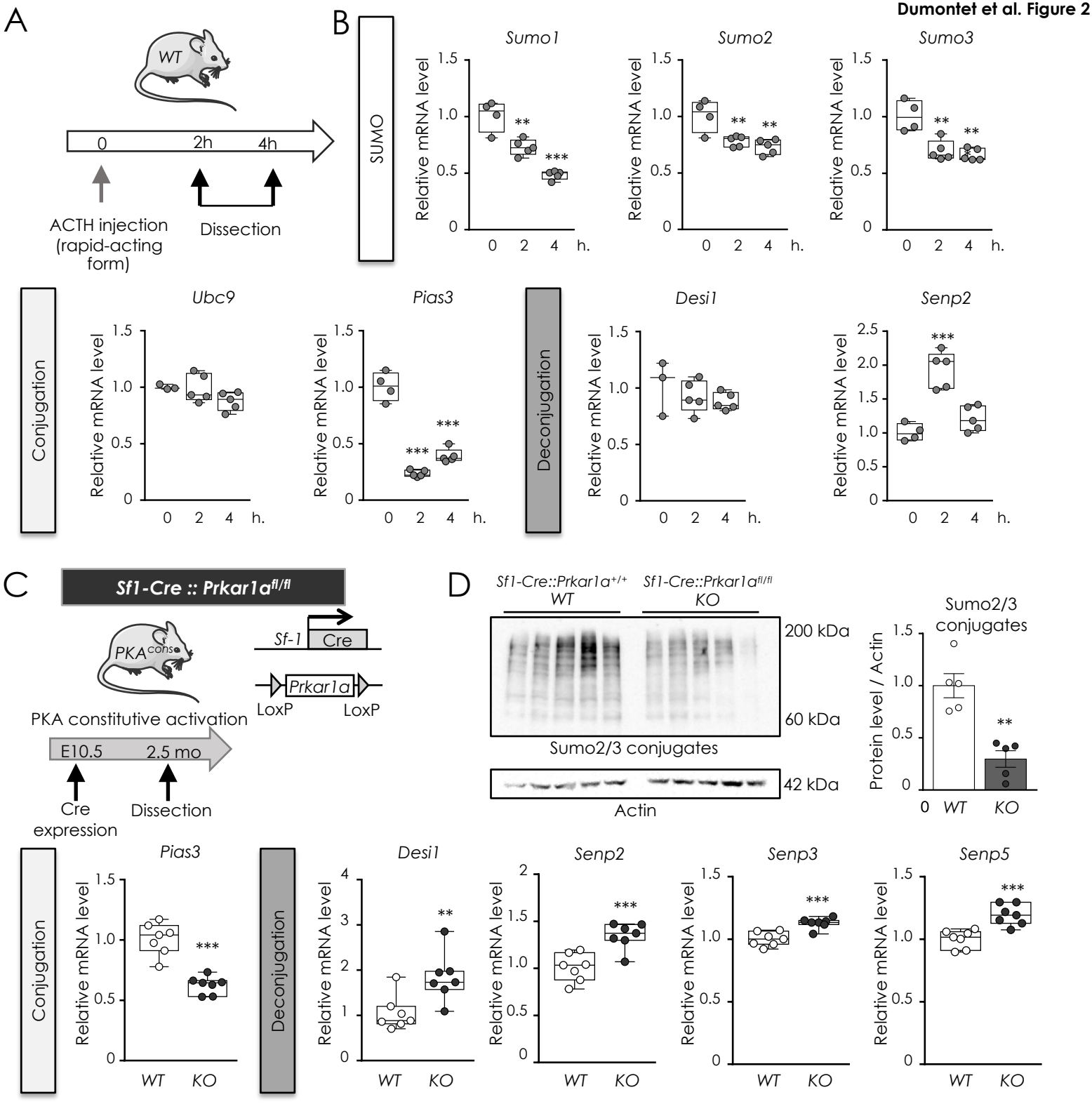
A
WT
0
2h
4h
ACTH injection (rapid-acting form)
Dissection
B
SUMO
Sumo1
Sumo2
Sumo3
Relative mRNA level
h.
Conjugation
Ubc9
Pias3
Deconjugation
Desi1
Senp2
C
Sf1-Cre :: Prkar1a fl/fl
PKA cons
Sf-1
Cre
Prkar1a
LoxP
LoxP
PKA constitutive activation
E10.5
2.5 mo
Cre expression
Dissection
D
Sf1-Cre::Prkar1a +/+
WT
Sf1-Cre::Prkar1a fl/fl
KO
200 kDa
60 kDa
Sumo2/3 conjugates
42 kDa
Actin
Sumo2/3 conjugates
Protein level / Actin
Conjugation
Pias3
Deconjugation
Desi1
Senp2
Senp3
Senp5
WT
KO

Fig. 2. Acute hormonal induction or constitutive activation of PKA signalling affect protein SUMOylation and SUMO pathway gene expression in mouse adrenals. *A-B*) Wild-type mice were injected with immediate ACTH and adrenals were removed 2h or 4h later, control adrenals were dissected from untreated mice (0h) and subjected to RNA extraction. *A*) Experimental setup. *B*) RT-qPCR analyses of SUMOylation pathway gene expression normalised with respect to *Actin* gene expression. Statistical analyses were conducted by 1-way ANOVA followed by Dunett's test. *C-D*) Carney complex mouse model with constitutive activation of PKA following adrenal inactivation of *Prkar1a* (*Sf1-Cre::Prkar1a*$^{fl/fl}$ mice). *C*) Experimental setup. Adrenals from *Sf1-Cre::Prkar1a*$^{+/+}$ (*WT*) and *Sf1-Cre::Prkar1a*$^{fl/fl}$ (*KO*) mice were removed and subjected to RNA and protein extraction. RT-qPCR analyses of SUMOylation pathway gene expression normalised with respect to *Actin* gene expression and, *D*) western blot analyses of Sumo2/3 conjugates in adrenal protein extracts and quantification (histogram). Tubulin signal was used to normalise the quantification of SUMO signals. Statistical analyses were conducted by Student t-test. Quantification histograms represent mean ± SEM. *p<0.05; **p<0.01; ***p<0.001.

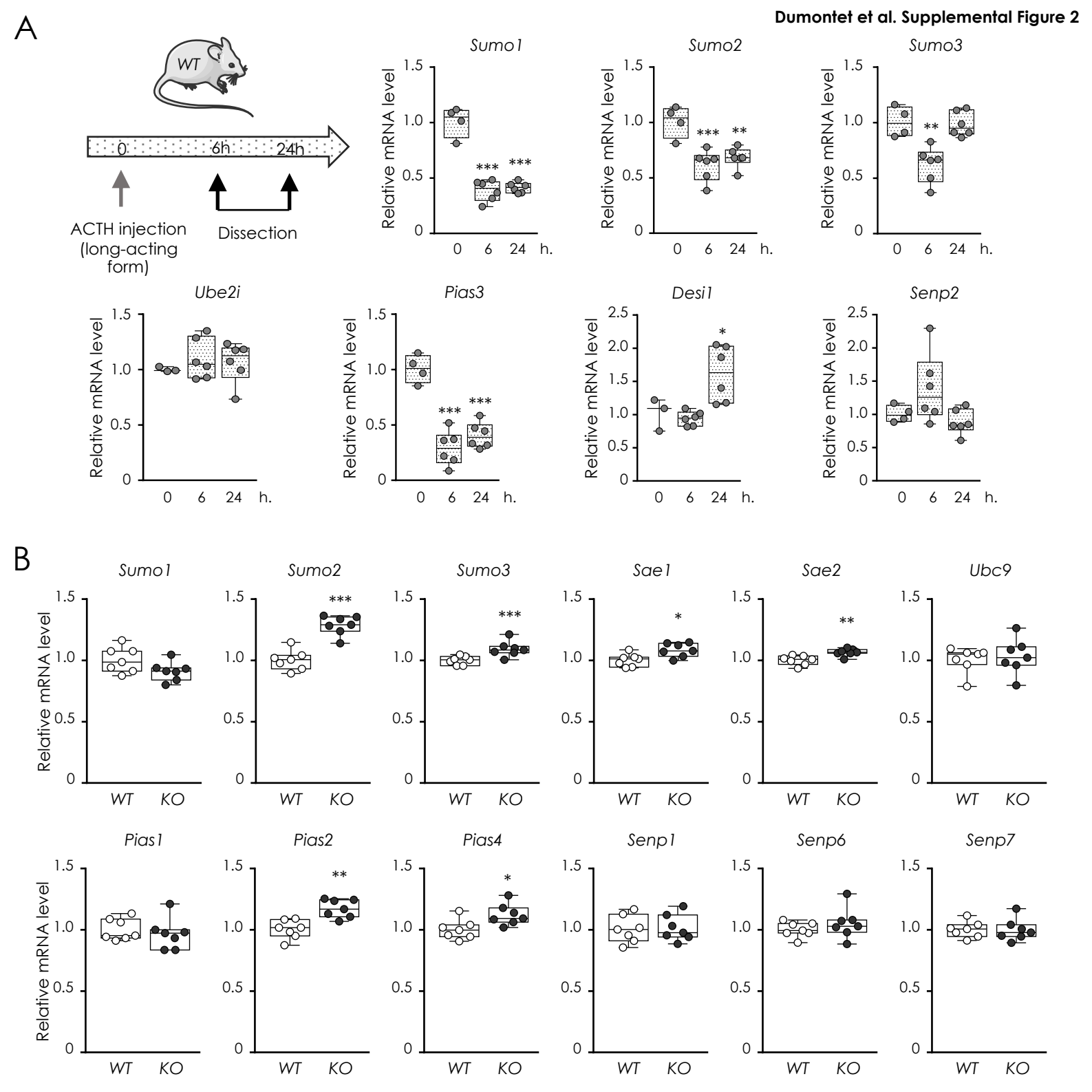
A
WT
0
6h
24h
ACTH injection (long-acting form)
Dissection
Sumo1
Sumo2
Sumo3
Ube2i
Pias3
Desi1
Senp2
Relative mRNA level
h.
B
Sumo1
Sumo2
Sumo3
Sae1
Sae2
Ubc9
Pias1
Pias2
Pias4
Senp1
Senp6
Senp7
WT
KO

Supplemental Fig. S2. *A*) Wild-type mice were injected with retard ACTH and adrenals were removed after 6h or 24h, control adrenals were dissected from untreated mice (0h) and subjected to RNA extraction. Experimental setup. RT-qPCR analyses of SUMOylation pathway gene expression normalised with respect to *Actin* gene expression. Statistical analyses were conducted by 1-way ANOVA followed by Dunett's test. *B*) Adrenals from *Sf1-Cre::Prkar1a*$^{+/+}$ (*WT) and Sf1-Cre::Prkar1a*$^{fl/fl}$ (*KO*) mice were removed and subjected to RNA extraction. RT-qPCR analyses of SUMOylation pathway gene expression normalised with respect to *Actin* gene expression. Statistical analyses were conducted by Student t-test. Quantification histograms represent mean ± SEM. *p<0.05; **p<0.01; ***p<0.005.

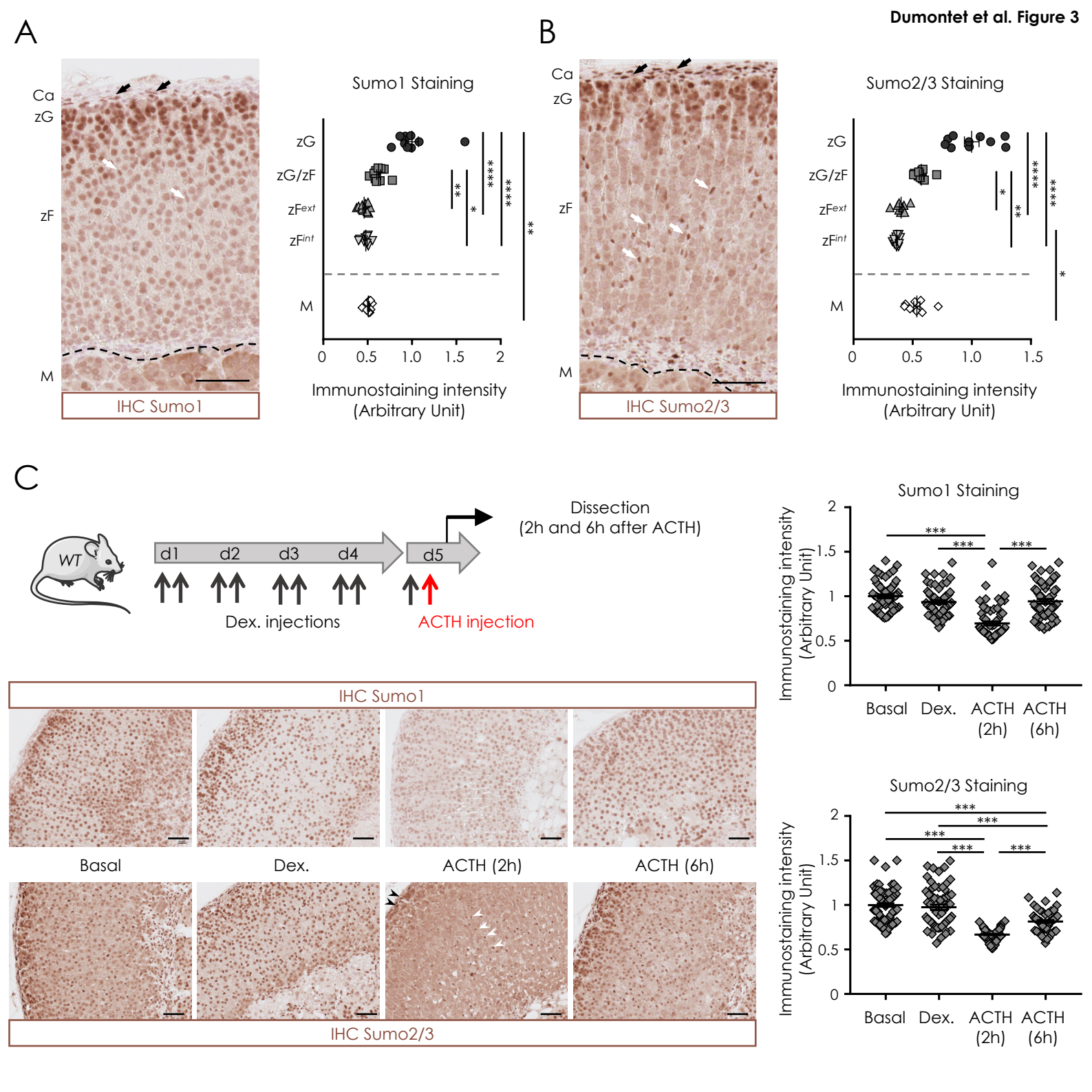
A
Ca
zG
zF
M
IHC Sumo1
Sumo1 Staining
zG
zG/zF
zF^ext
zF^int
M
0
0.5
1.0
1.5
2
Immunostaining intensity
(Arbitrary Unit)
B
Ca
zG
zF
M
IHC Sumo2/3
Sumo2/3 Staining
zG
zG/zF
zF^ext
zF^int
M
0
0.5
1.0
1.5
Immunostaining intensity
(Arbitrary Unit)
C
WT
d1
d2
d3
d4
d5
Dissection
(2h and 6h after ACTH)
Dex. injections
ACTH injection
IHC Sumo1
Basal
Dex.
ACTH (2h)
ACTH (6h)
IHC Sumo2/3
Sumo1 Staining
Immunostaining intensity
(Arbitrary Unit)
Basal
Dex.
ACTH (2h)
ACTH (6h)
Sumo2/3 Staining
Immunostaining intensity
(Arbitrary Unit)
Basal
Dex.
ACTH (2h)
ACTH (6h)

Fig. 3. SUMOylation is regionalised in mouse adrenal cortex and modulated by ACTH/PKA signalling. *A-B*) SUMOylation profile forms a decreasing gradient of intensity from the outer to the inner cortex. The accumulation of conjugated proteins to Sumo1 (*A*) and Sumo2/3 (*B*) was analysed by immunohistochemistry in adrenals of 6-month-old female mice. The quantification graphs represent mean ± SEM of SUMO nuclear staining intensity in each histological zone and inter-zone all along the cortex and in medulla, for 3 adrenals from 3 different animals and 50-60 nuclei per adrenal. Statistical analyses were conducted by Kruskal-Wallis followed by Dunn's test. Ca: capsule; zG: zona glomerosa; zF^{ext}: external zona fasciculata; zF^{int}: internal zona fasciculata; M: medulla. *C*) Stimulation of the corticotropic axis changes the cortical SUMOylation profile. Six-month-old female mice were treated with dexamethasone (Dex.) for 5 days, injected or not the last morning with ACTH and sacrificed 2h or 6h later. Basal conditions correspond to untreated mice. The accumulation of conjugated nuclear proteins to Sumo1 and Sumo2/3 was analysed by immunohistochemistry. The quantification graphs represent mean ± SEM of SUMO nuclear staining intensity in zF cells for 6 adrenals from 6 different animals and 10 nuclei per adrenal. Black and white arrows: nuclear Sumo staining in capsular and endothelial cells, respectively. Statistical analyses were conducted by 1-way ANOVA followed by Tukey post hoc test. *p<0.05, **p<0.01, ***p<0.001, ****p<0.0001. Scale bars = 50 µm.

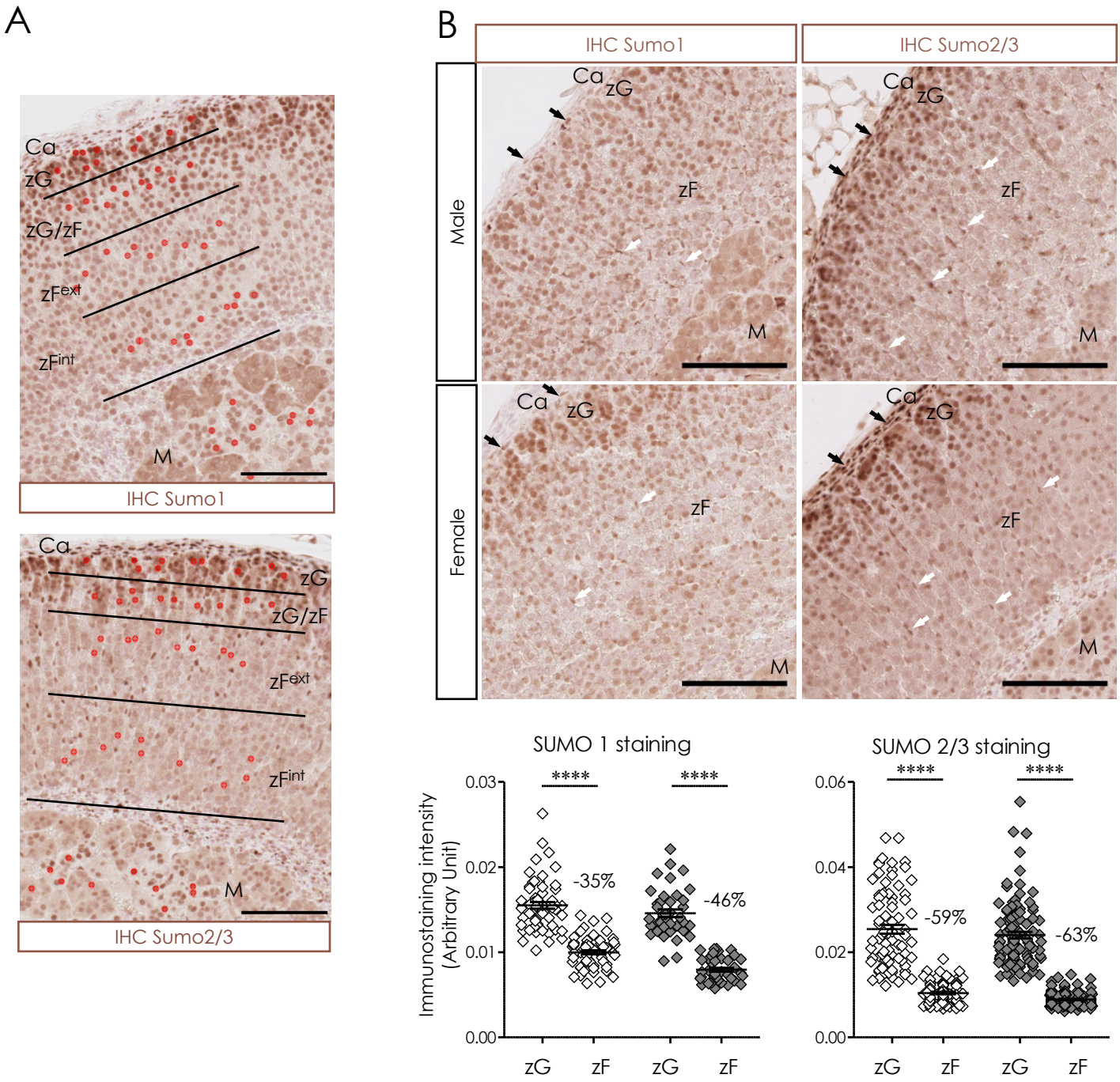
A
Ca
zG
zG/zF
zF^ext
zF^int
M
IHC Sumo1
Ca
zG
zG/zF
zF^ext
zF^int
M
IHC Sumo2/3
B
IHC Sumo1
IHC Sumo2/3
Male
Female
Ca
zG
zF
M
SUMO 1 staining
SUMO 2/3 staining
Immunostaining intensity (Arbitrary Unit)
0.03
0.02
0.01
0.00
0.06
0.04
****
-35%
-46%
-59%
-63%
zG
zF

Supplemental Fig. S3. SUMOylation is regionalised in mouse adrenal cortex from both female and male mice. The accumulation of conjugated proteins to Sumo1 and Sumo2/3 was analysed by immunohistochemistry in adrenals of 6-month-old mice. *A)* SUMOylation profile forms a decreasing gradient of intensity from the outer to the inner cortex. Pictures of Sumo1 and Sumo2/3 immunostaining illustrating the delimitation of zones and inter-zones chosen for quantification of nuclear staining intensity in Fig. 3. Ten nuclei (red dots) were analysed per area. *B*) Sumo1 and Sumo2/3 immunostaining patterns were compared in adrenals from 4 male and 5 female mice. The quantification graphs represent mean ± SEM of SUMO nuclear staining intensity in zG and zF from male (white lozenge) and female (grey lozenge) mice (20 nuclei per adrenal zone). Percentage decrease of SUMO staining between zG and zF was indicated for both sexes. Ca: capsule; zG: zona glomerosa; zF^{ext}: external zona fasciculata; zF^{int}: internal zona fasciculata; M: medulla. Black and white arrows: nuclear Sumo staining in capsular and endothelial cells, respectively. Statistical analyses were conducted by Mann-Whitney test. ****$p<0.0001$. Scale bars = 100µm.

C

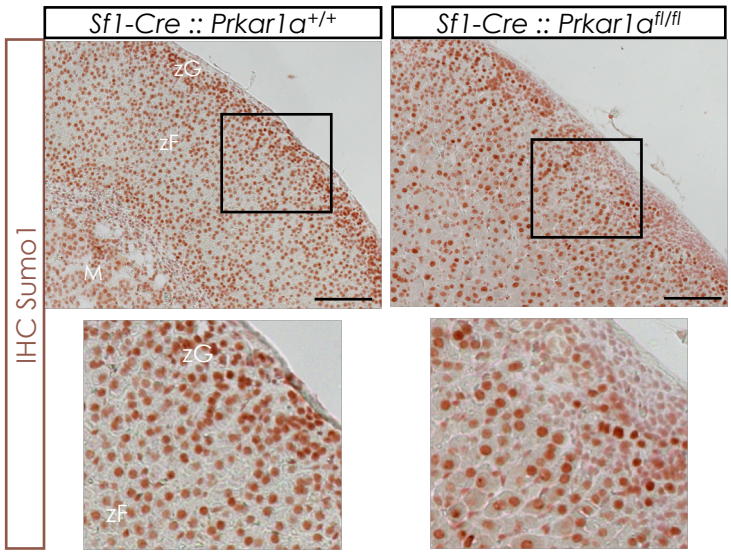
Sf1-Cre :: Prkar1a+/+
Sf1-Cre :: Prkar1afl/fl
IHC Sumo1
zG
zF
M
zG
zF

D

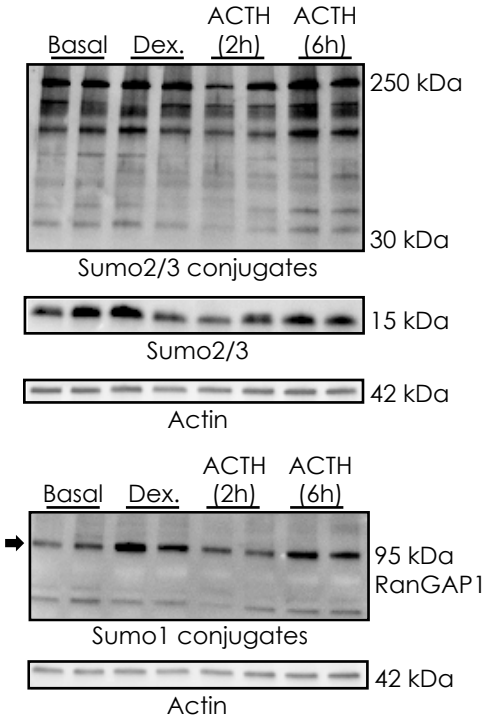
Basal
Dex.
ACTH (2h)
ACTH (6h)
250 kDa
30 kDa
Sumo2/3 conjugates
15 kDa
Sumo2/3
42 kDa
Actin
95 kDa
RanGAP1
Sumo1 conjugates

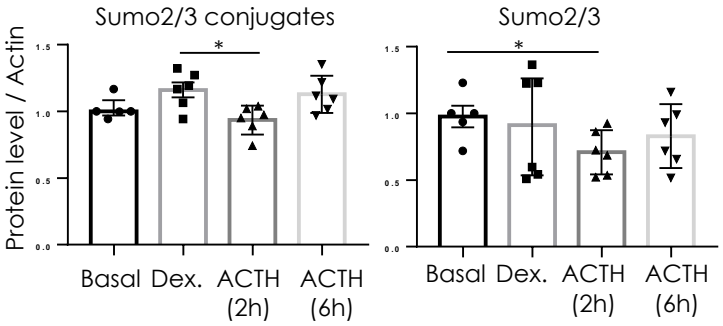
Sumo2/3 conjugates
Sumo2/3
Protein level / Actin
Basal
Dex.
ACTH (2h)
ACTH (6h)
*

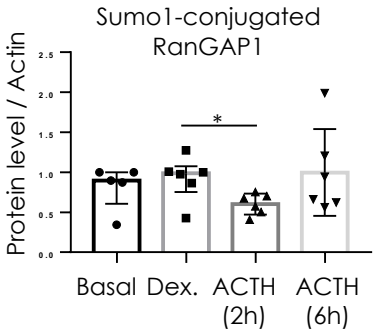
Sumo1-conjugated RanGAP1
Protein level / Actin
Basal
Dex.
ACTH (2h)
ACTH (6h)
*

Supplemental Fig. S3. SUMOylation is regionalised in mouse adrenal cortex and modulated by ACTH/PKA signalling. *C)* SUMOylation gradient is lost in the adrenal cortex of mouse model for Carney complex. The accumulation of conjugated nuclear proteins to Sumo1 was analysed by immunohistochemistry in 2.5 months female mice with adrenal invalidation of *Prkar1a* (*Sf1-Cre::Prkar1a$^{fl/fl}$*) and compared to control mice (*Sf1-Cre::Prkar1a$^{+/+}$*). *D*) Stimulation of the corticotropic axis changes the cortical SUMOylation profile. Six-month-old female mice were treated with dexamethasone (Dex.) for 5 days, injected or not the last morning with ACTH and sacrificed 2h or 6h later. Basal conditions correspond to untreated mice. The accumulation of Sumo2/3 conjugates, unconjugated Sumo2/3 and Sumo1-conjugated RanGAP1 (arrow) was analysed by western blot (representative Fig.) and quantified (histograms). Actin signal was used to normalise the quantification of SUMO signals. Histograms represent mean ± SEM. Statistical analyses were conducted by Mann-Whitney test. *p<0.05. zG: zona glomerosa; zF: zona fasciculata; M: medulla. Scale bars = 100 µm.

A

IHC SUMO1

P1 : *Control adrenal*

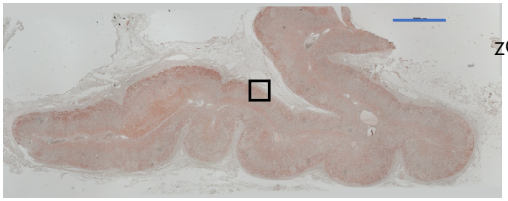

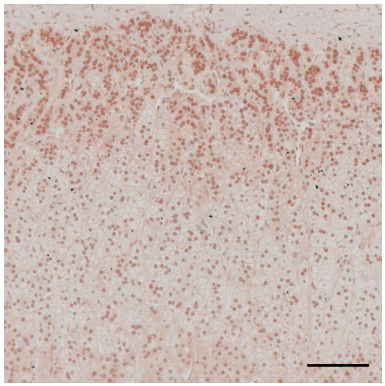

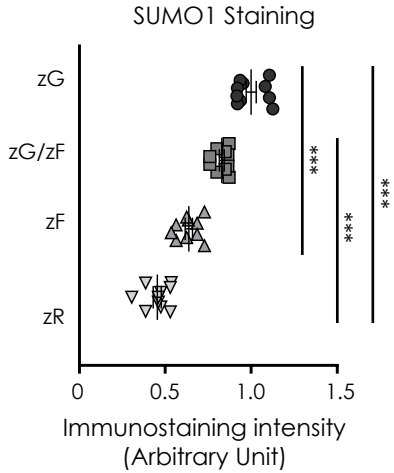

B

IHC SUMO1

P2 : *PPNAD (PRKAR1A germinal mutation, LOH in nodules)*

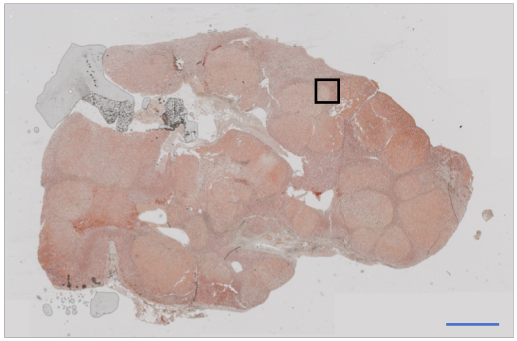

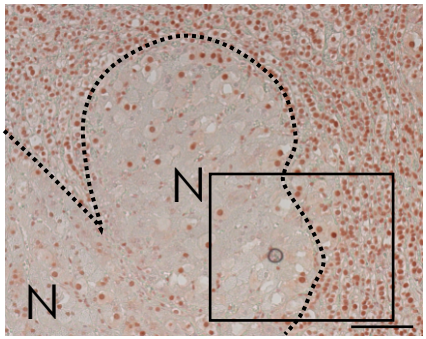

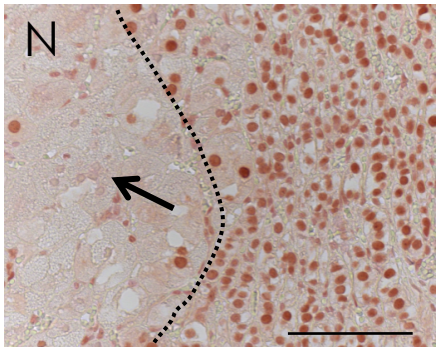

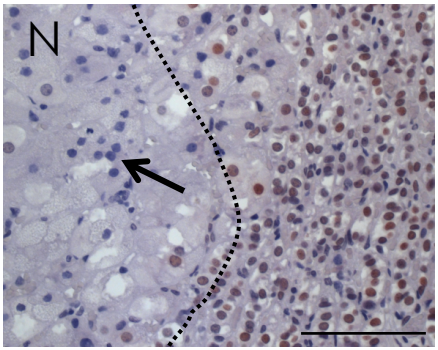

H&E staining

C

IHC SENP1

P3 : *PPNAD (PRKAR1A germinal mutation, LOH in nodules)*

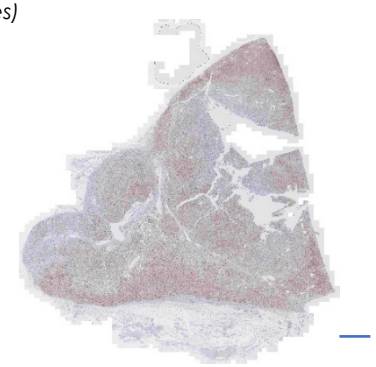

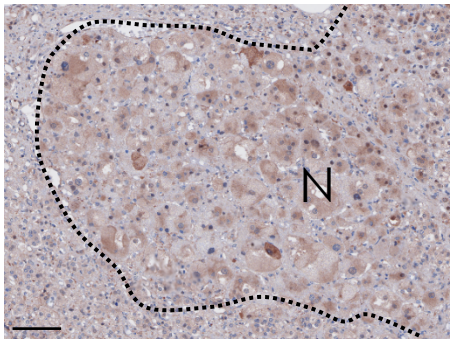

H&E staining

Fig. 4. SUMOylation is regionalized in human adrenal cortex and altered in nodular hyperplasia from Carney complex patients. *A*) SUMOylation profile forms a decreasing gradient of intensity from the outer to the inner cortex. The accumulation of conjugated proteins to SUMO1 was analysed by immunohistochemistry in a control human adrenal. The quantification graph represents mean ± SEM of SUMO1 nuclear staining intensity in steroidogenic cells in each histological zone and inter-zone all along the cortex. Statistical analyses were conducted by 1-way ANOVA followed by Dunett's test. ***p<0.001. zG: zona glomerosa, zF: zona fasciculata; zR: zona reticularis. *B-C*) HypoSUMOylation of PPNAD nodules. PPNAD sections from patients with *PRKAR1A* germinal mutation were immunostained for SUMO1 (*B*) or for SENP1 (*C*) and counterstained with hematoxylin (H&E). HypoSUMOylated nuclei (black arrow). N: nodule. Blue scale bars = 2 cm, black scale bars = 100 µm.

A

IHC SUMO1 | IHC SUMO2/3

P1 : *Control adrenal*

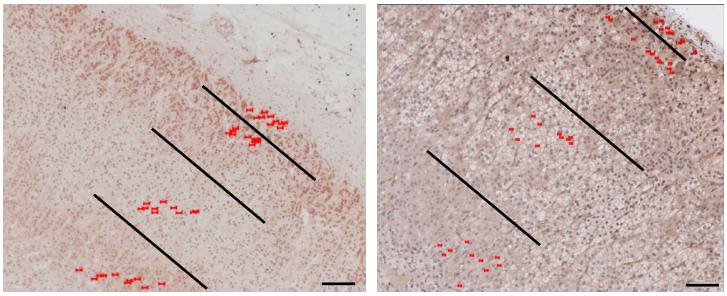

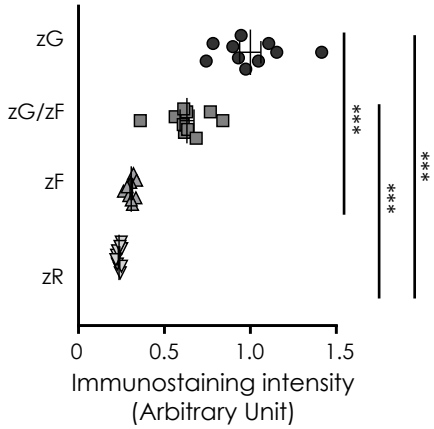

B

IHC SUMO1

P4 : *PPNAD (PRKAR1A germinal mutation, LOH in nodules)*

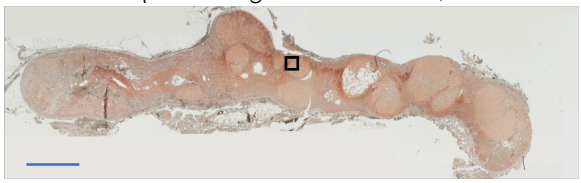

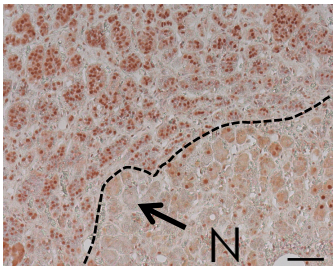

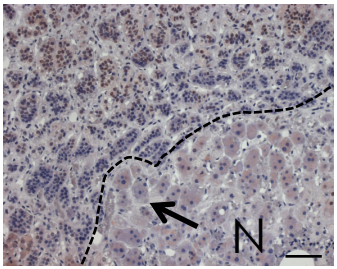

P5 : *PPNAD (PRKAR1A germinal mutation, LOH in nodules)*

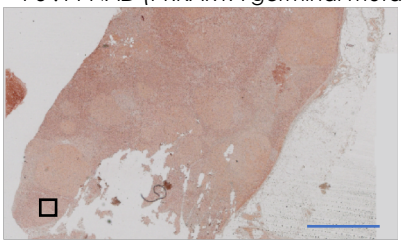

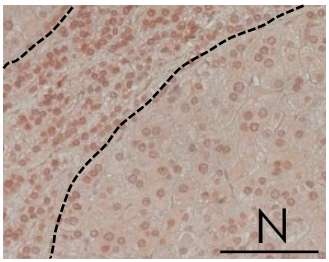

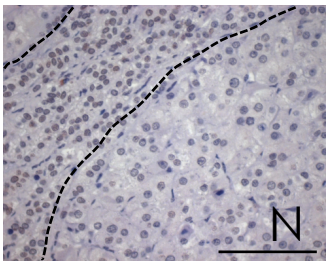

C

IHC SENP1

P6 & P7 : *PPNADs (no PRKAR1A mutation)*

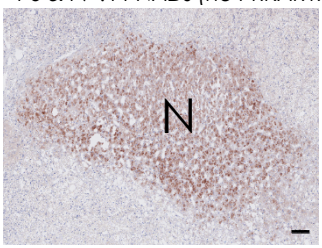

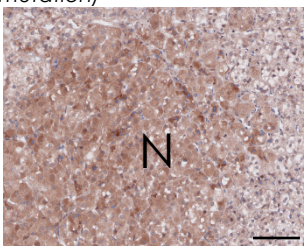

Supplemental Fig. S4. SUMOylation is regionalized in human adrenal cortex and altered in nodular hyperplasia from Carney complex patients. *A*) Pictures of SUMO1 and SUMO2/3 immunostaining illustrating the delimitation of zones and inter-zones chosen for quantification of nuclear staining intensity in Fig. 4. Ten nuclei (red dots) were analysed per area. The quantification graph represents mean ± SEM of SUMO2/3 nuclear staining intensity in steroidogenic cells in each histological zone and inter-zone all along the cortex. Statistical analyses were conducted by 1-way ANOVA followed by Dunett's test. ***p<0.001. zG: zona glomerosa, zF: zona fasciculata; zR: zona reticularis. *B-C*) HypoSUMOylation of PPNAD nodules. PPNAD sections from patients with *PRKAR1A* germinal mutation or carrying unknown mutation were immunostained for SUMO1 (*B*) or for SENP1 (*C*) and counterstained with hematoxylin (H&E). HypoSUMOylated nuclei (black arrow). N: nodule. Blue scale bars = 2 cm, black scale bars = 100 µm.

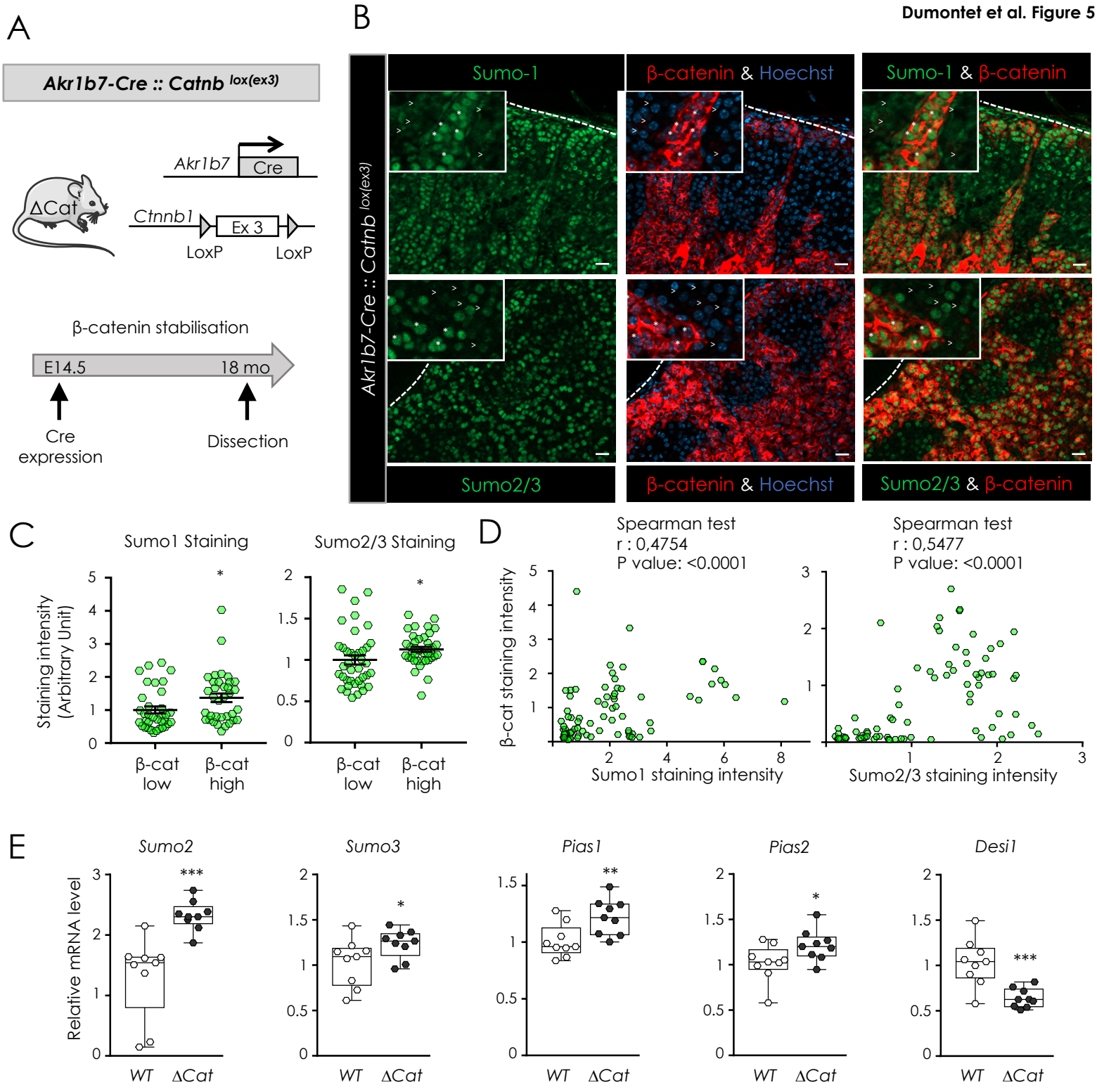
A
Akr1b7-Cre :: Catnb lox(ex3)
Akr1b7
Cre
ΔCat
Ctnnb1
Ex 3
LoxP
LoxP
β-catenin stabilisation
E14.5
18 mo
Cre expression
Dissection
B
Akr1b7-Cre :: Catnb lox(ex3)
Sumo-1
β-catenin & Hoechst
Sumo-1 & β-catenin
Sumo2/3
β-catenin & Hoechst
Sumo2/3 & β-catenin
C
Sumo1 Staining
Sumo2/3 Staining
Staining intensity (Arbitrary Unit)
β-cat low
β-cat high
β-cat low
β-cat high
D
Spearman test
r : 0,4754
P value: <0.0001
Spearman test
r : 0,5477
P value: <0.0001
β-cat staining intensity
Sumo1 staining intensity
Sumo2/3 staining intensity
E
Sumo2
Sumo3
Pias1
Pias2
Desi1
Relative mRNA level
WT
ΔCat

Fig. 5. Adrenal cortex SUMOylation is enhanced by constitutive activation of WNT/β-catenin signalling. *A*) Experimental setup. β-catenin stabilization in adrenal cortex was allowed by deletion of exon 3 of *Ctnnb1 (Catnb$^{lox(ex3)}$ allele)* using *Akr1b7-Cre* line (referred to as ΔCat mice). *B*) Coimmunofluorescent labeling of Sumo1 (upper) or Sumo2/3 (bottom) (green), β-catenin (red) and merged signals, in adrenal sections from ΔCat female mice of 18 months. *Inset*, magnification view showing nuclei from cells with low (white arrowheads) or high (white asterisk) β-catenin staining. Scale bars = 20 µm. *C*) The quantification graphs represent mean ± SEM of SUMO nuclear Sumo1 and Sumo2/3 staining intensity in cells that express low or high levels of β-catenin (3 adrenals from 3 different animals and 10-15 nuclei per adrenal). *D*) Sumo1 or Sumo2/3 nuclear staining is correlated with β-catenin activation. Spearman correlation between staining intensity values of Sumo1 or Sumo2/3 nuclear signal and staining intensity of β-catenin nucleo-cytoplasmic signal. r: Spearman correlation coefficient. *E*) Adrenals from *Akr1b7-Cre::Catnb$^{+/+}$ (WT)* and *Akr1b7-Cre::Catnb$^{lox(ex3)/+}$* (*ΔCat*) mice were removed and subjected to RNA extraction. RT-qPCR analyses of SUMOylation pathway gene expression normalised with respect to *Actin* gene expression. Statistical analyses were conducted by Student t-test. Quantification histograms represent mean ± SEM. *p<0.05, **p<0.01, ***p<0.001

A

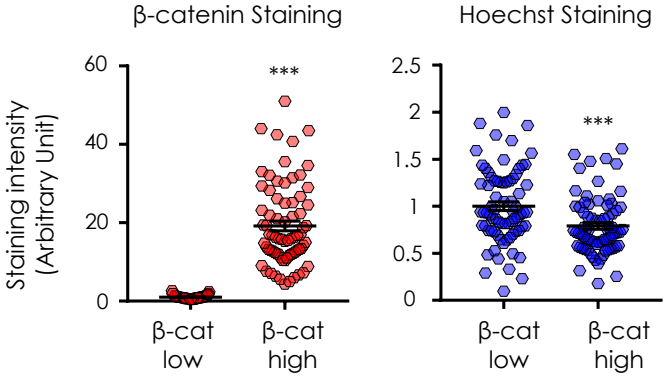
β-catenin Staining
Hoechst Staining
Staining intensity (Arbitrary Unit)
60
40
20
0
***
2.5
2
1.5
1
0.5
0
***
β-cat low
β-cat high
β-cat low
β-cat high

B

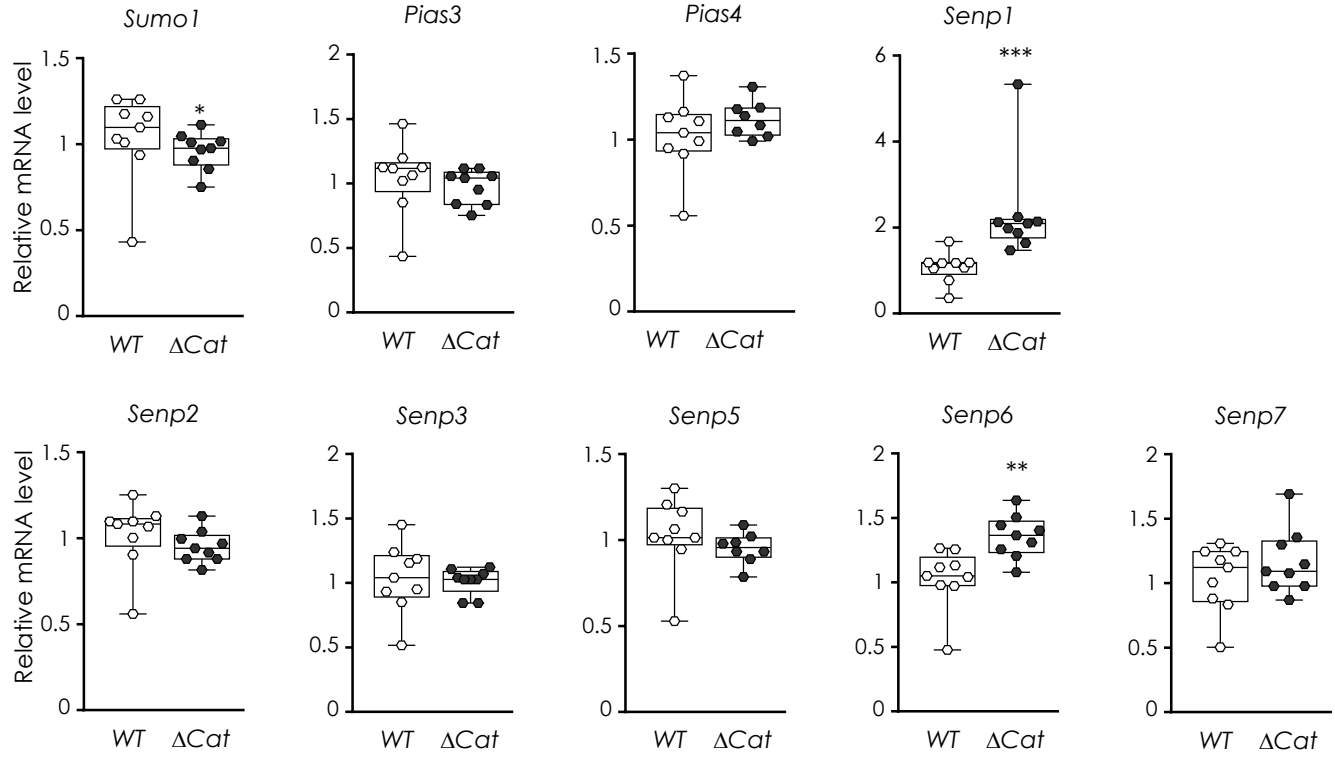
Sumo1
Pias3
Pias4
Senp1
Relative mRNA level
1.5
1
0.5
0
*
2
1.5
1
0.5
0
1.5
1
0.5
0
6
4
2
0
***
WT
ΔCat
Senp2
Senp3
Senp5
Senp6
Senp7
Relative mRNA level
**
WT
ΔCat

Supplemental Fig. S5. Adrenal cortex SUMOylation is enhanced by constitutive activation of WNT/β-catenin signalling. *A*) Assessment of β-catenin activation in ΔCat adrenal cortex by measuring β-catenin immunostaining. The quantification graphs represent mean ± SEM of nucleo-cytoplasmic β-catenin staining intensity in tumour cortex areas that have recombined $Catnb^{lox(ex3)}$ allele (β-cat high) or in intact non-recombinant cortex (β-cat low). As a control, Hoescht staining intensity was quantified in cells from the same areas (3 adrenals from 3 different animals and 10-15 nuclei per adrenal). *B*) Adrenals from *Akr1b7-Cre::*$Catnb^{+/+}$ *(WT)* and *Akr1b7-Cre::*$Catnb^{lox(ex3)/+}$ (*ΔCat*) mice were removed and subjected to RNA extraction. RT-qPCR analyses of SUMOylation pathway gene expression normalised with respect to *Actin* gene expression. Statistical analyses were conducted by Student t-test. Quantification histograms represent mean ± SEM. *p<0.05, **p<0.01, ***p<0.001.

Supplemental Table S1A. Western blot conditions

Target	Reference	Size	Provider	Isotype	Dilution
Sumo1	4930	Profile	Cell Signaling	Rabbit	1/1000
Sumo2/3	SAB4200190	Profile	Sigma-Aldrich	Rat	1/1000
Sumo2/3 (Fig. S3D)	ab3742	Profile	Abcam	Rabbit	1/1000
Senp2	267075	68 kDa	Santa-Cruz	Rabbit	1/2000
Ube2i	75854	18 kDa	Abcam	Rabbit	1/10000
Tubulin	T6074	50 kDa	Sigma-Aldrich	Mouse	1/25 000
Actin	2066	42 kDa	Sigma-Aldrich	Rabbit	1/10 000

Supplemental Table S1B : Sequences of the primers used in RTqPCR

Target	Forward	Reverse
mm *Sumo1*	5'-ATTGGACAGGATAGCAGTGAGA-3'	5'-TCCCAGTTCTTTCGGAGTATGA-3'
mm *Sumo2*	5'-ACTAATGAAAGCCTATTGTGAAC-3'	5'-TGGAGTAAAGTAGCAGGCTCCCTTT-3'
mm *Sumo3*	5'-GCTGATGAAGGCCTACTGTGAGA-3'	5'-GGTGTGGGGACGCTCCCTCG-3'
mm *Sae1*	5'-CTGCCCCCGACTACTTTCTG-3'	5'-CCAGGGAGTCAAACACGTCA-3'
mm *Sae2*	5'-AAGAACCTGGTGCTCACTGG-3'	5'-TTGGCAACCTGAGCCTTTGA-3'
mm *Ubc9*	5'-AAGGGGACTCCATGGGAAGG-3'	5'-CTCCAGGATGGACAGGCACA-3'
mm *Pias1*	5'-GCTCGTGGGCTCCAATGA-3'	5'-CTGGTTGTGGGACGCTACCT-3'
mm *Pias2*	5'-GAAGACCCTCCCGCCAAAAG-3'	5'-ACACTGGGCACCCTTACAGA-3'
mm *Pias3*	5'-CTGCGCGAGCCCTTTCT-3'	5'-TGGAGCTCAGACACTCGGAA-3'
mm *Pias4*	5'-ATGTGCCCTGTGTGTGACAA-3'	5'-CCTTCCGCCAGGAACTCAAT-3'
mm *Senp1*	5'-CTACAAGAAGCCCAGCCTATCGTC-3'	5'-GTCACCTGAGCCAAGGAAACTG-3'
mm *Senp2*	5'-AACAGTCTCTACAATGCTGCCA-3'	5'-CCGTGTTCCATTACAAGCAGAA-3'
mm *Senp3*	5'-GATGGACTAAGGTGGACCCC-3'	5'-ATGAGTATGCTGGCATCAGGG-3'
mm *Senp5*	5'-GGATGGGCAGAACTGGTTGA-3'	5'-GTGGACCTTGTCTGGGACTG-3'
mm *Senp6*	5'-ACGTGCCAGGACATTTGTGA-3'	5'-TCTTCAAGCAGCTTCCCACC-3'
mm *Senp7*	5'-AGATCCTCTTCACCAAAGCCTTA-3'	5'-TCTTCCTAATTCTGTTTGCCGGA-3'
mm *Desi1*	5'-TTCGGCAGCAGCGGTATTTC-3'	5'-CTCCTCGGAACAGAGACTCC-3'
mm *Actin*	5'-TCATCACTATTGGCAACGAGC-3'	5'-AGTTTCATGGATGCCACAGG-3'
mm *Akr1b7*	5'-GGCTGCCATTCTCAGCTTCAACAG-3'	5'-GCAAGTGGACCTCAGTATTCCTCG-3'

Supplemental Table S1C. Immunohistochemical and immunohistofluorescence conditions

Target	Reference	Provider	Isotype	Dilution	Epitope Retrival (25 min, boiling in solution)	Saturation conditions	Secondary	Revelation
Sumo1	4930	Cell Signaling	Rabbit	1/1000	Vector solution (H330, Vector Labs)	NGS 1.5%	ImPRESS HRP (Peroxydase) polymere detection kit (vectors labs) during 30 min. at room temperature	Novared Kit (Abcys) or TSA Kit (Alexa 488 and 555) (Invitrogen)
Sumo2/3	ab3742	Abcam	Rabbit	1/1000	Citrate de sodium 10mM, pH 6 /Tween 0.05%	NGS 1.5%		
β-catenin	610153	BD Biosciences	mouse	1/500	Citrate de sodium 10mM, pH 6 /Tween 0.05% or Vector solution (H330, Vector Labs)	BSA 1%		
Senp1	108981	Abcam	Rabbit	1/100	Tris 10mM EDTA 1mM pH 9.0	NGS 1.5%		